2021

CHARACTERIZATION OF OVARIAN TISSUE CULTURE AND INVESTIGATION OF EMBRYONIC RESPONSE TO TEMPERATURE STRESS USING A SHP2 PHOSPHATASE INHIBITOR IN CIONA INTESTINALIS

Rose Jacobson
University of Rhode Island, rose_jacobson@uri.edu

CHARACTERIZATION OF OVARIAN TISSUE CULTURE AND INVESTIGATION OF EMBRYONIC RESPONSE TO TEMPERATURE STRESS USING A SHP2 PHOSPHATASE INHIBITOR IN CIONA INTESTINALIS

BY

ROSE JACOBSON

A DISSERTATION SUBMITTED IN PARTIAL FULFILLMENT OF THE

REQUIREMENTS FOR THE DEGREE OF

DOCTOR OF PHILOSOPHY

IN

BIOLOGICAL AND ENVIRONMENTAL SCIENCES

UNIVERSITY OF RHODE ISLAND

2021

DOCTOR OF PHILOSOPHY DISSERTATION

OF

ROSE JACOBSON

APPROVED:

Dissertation Committee:

Major Professor Steven Irvine

Niall Howlett

Becky Sartini

Hollie Putnam

Brenton DeBoef
DEAN OF THE GRADUATE SCHOOL

UNIVERSITY OF RHODE ISLAND

2021

ABSTRACT

This dissertation is comprised of two parts, the first is cell culture. In this work I describe the successful primary culture of *Ciona intestinalis* ovary tissue. Improved cell proliferation in 3D Petri Dish® system over culture treated plastic is shown, as well as the efficacy of using *C. intestinalis* hemolymph as a media additive. The seeded ovarian cells assemble into multicellular aggregations, which mimic the morphology of *in vivo* ovaries. It is also important to understand the molecular pathways in which marine organisms handle stress and how these pathways change in high stress situations.

The second is the role of Shp2 in temperature stress. It is projected that ocean temperatures may raise as much as 4°C over the next century, and there is very little known about how this increase in temperature will affect both reproduction and embryonic development in marine organisms. In this work I also describe the phenotypic abnormalities which occur during embryogenesis in *Ciona intestinalis* when Shp2 protein tyrosine phosphatase is inhibited. The phenotypic abnormalities are consistent with the abnormalities observed in *C. intestinalis* embryos reared at high temperatures stress. This suggests that Shp2 is an important protein in the amelioration of stress in developing *C. intestinalis* embryogenesis and is required for normal embryogenesis.

ACKNOWLEDGMENTS

I would like to thank my advisor, Dr. Steven Irvine, for all his help and support during my dissertation work. I would also like to thank my dissertation committee members, Dr. Niall Howlett, Dr. Hollie Putnam, and Dr. Becky Sartini for their guidance and advice throughout my dissertation work. I would like to thank Dr. Jeffrey Morgan for allowing use of his 3D Petri Dishes® for the cell culture work. I would like to thank Dr. Jackie Webb for teaching me how to prepare the histological materials as well as for the use of her equipment in that process. I would like to thank the Rhode Island Science and Technology Advisory Council, the URI Council for Research, and the Enhancement of Graduate Research Award for funding my dissertation work.

DEDICATION

I would like to dedicate my dissertation to my aunt, Rhea Gage, who lost her battle with Multiple Sclerosis on March 4th, 2021. As I look back on my time working on this dissertation, I realized that somewhere along the way I lost my "why". Why did I choose to continue my education? What was it that drove me to science? What is my passion? What is my purpose? With her passing I was reminded that I chose this path to make a difference, even if only for one person. I went into research and continued my education because I did not understand her disease and research has become my passion. During my time working on my dissertation, I was given the opportunity to teach and found my purpose. It was a blessing to love such a strong, independent, and brave woman who has inspired me and helped me find both my passion and purpose.

PREFACE

As I look back on my time working on my dissertation, I am extremely grateful for all of the experiences I have had and everything that I have learned. I began my graduate career at the University of Rhode Island unsure of what I wanted to do other than learn. I had the opportunity to rotate in three very unique labs during my first two semesters. I ultimately decided to complete my dissertation research with Dr. Steven Irvine where I learned a lot about both experimental techniques as well as training other researchers. During my dissertation work I have also had the opportunity to teach multiple courses, both teaching labs and lecture courses. Throughout this time, I have become much more confident in my abilities both in the lab and in the classroom.

TABLE OF CONTENTS

LIST OF TABLES

TABLE PAGE

LIST OF FIGURES

Chapter 1: 3D Ovarian Tissue Culture using *Ciona intestinalis*

1.1 Introduction

Tissue Culture

Tissue culture is one of the most important tools used in biochemistry, cell biology, and cell physiology research. Tissue culture allows for research in all of these fields to be done *in vitro,* making complex biological systems more experimentally tractable. In the present study I focused on using the model chordate *Ciona intestinalis* to generate a marine invertebrate tissue culture. *C. intestinalis,* an ascidian in the subphylum Urochordata, was chosen as the organism of interest because of its emerging importance for functional genomics and developmental biology (N Satoh and Levine 2005; Stolfi and Christiaen 2012).

To date there are many different vertebrate tissue culture lines available. Among invertebrates, many insect cell culture lines have been established, but there are no established cell culture lines for marine invertebrates. As for primary cultures, a number of studies have been published for various marine invertebrates (Cai and Zhang 2014; Baruch Rinkevich 2011; B Rinkevich 1999). Focusing on ascidians, there has been much interest in tissue culture in colonial ascidians, because of their ability to develop from asexual buds, which has implications for stem cell biology (Duckworth et al. 2004; Kawamura and Fujiwara 1995; Kawamura et al. 2006; B Rinkevich and Rabinowitz 1993; 1997; Rabinowitz and Rinkevich 2004). Of the over 3,000 species of tunicates, there are 35 publications on stem cells and 80 publications on cell culture (Rosner et al. 2021), although many of these are in

colonial ascidians. Marine invertebrate cell culture provides a promising advancement in the assessment of impacts of ocean acidification, increasing ocean temperatures, and ecotoxicological impacts of pollutants (Rosner et al. 2021).

In solitary ascidians, such as *C. intestinalis,* there have been very few published papers on cell or tissue culture but it has been reported for nervous system cells (Zanetti et al. 2007), pharynx (Raftos, Stillman, and Cooper 1990; Sawada, Zhang, and Cooper 1994; Arizza, Cooper, and Parrinello 1997), and hemocytes (Sawada, Zhang, and Cooper 1994; Peddie, Richest, and Smith 1995; Raftos, Stillman, and Cooper 1990; Arizza, Cooper, and Parrinello 1997). *Ciona* hemocytes in culture only showed proliferation for 3 days, after which cell began to die. When co-cultured with mammalian cells, the hemocytes showed cytotoxic activity towards the mammalian cells (Peddie, Richest, and Smith 1995). *Ciona* nervous system cells were cultured from larval stage embryos and were grown on culture treated glass. In this culture system, cell death began after 7 days and optimal growth of cells was seen for a maximum of 13 days. Electrophysiological analysis of nervous system cells showed that they were indeed neuronal cells (Zanetti et al. 2007).

In previous work in *Styela clava*, there has been tissue culture of both pharynx explants and hemocytes (Sawada, Zhang, and Cooper 1994; Raftos, Stillman, and Cooper 1990). The hemocytes alone did not proliferate in culture after the initial plating while pharynx explants survived multiple passing attempts for 72 days in culture. More than $1/4^{th}$ of the pharynx primary cultures became overrun by protists and were unusable after 24 days. During the 72 days the pharynx explants were in

culture, the tissue remained unchanged from its in vivo morphology with the exception that hemocytes had moved from the tissue into the media (Raftos, Stillman, and Cooper 1990). Another attempt at pharynx explant culture in *Styela clava* showed survival of the explants for 82 days in culture. In this culture system, it was also found that hemocytes has moved from the explants to become free in the culture media (Sawada, Zhang, and Cooper 1994). Analysis of *Styela clava* hemocytes released from phanyx explant cultures also showed the release of hemagglutinins which can cause agglutination of cells (Arizza, Cooper, and Parrinello 1997).

Traditional tissue culture methods rely on adhesion of cells to culture treated plastic for cell survival. This forces the cells to form unnatural adhesion to a flat plastic surface so that they are not washed away with media changes. This also means that when cells need to be passed and re-seeded or removed for experiments that chemicals must be used to degrade these adhesions. These methods also change the natural histology of the cells, meaning that it is less likely that the cells would behave the same way *in vivo*. In order to circumvent some of these problems with traditional tissue culture methods I explored the use of a "3D" tissue culture system (Napolitano et al. 2007). This approach is to grow the cells in non-adherent microwells so that cells may form more natural adhesions to each other and even self-assemble into "organoids" – three-dimensional cellular aggregations that may replicate the function of *in vivo* tissues (Achilli, Meyer, and Morgan 2012; Desroches et al. 2012; Morgan et al. 1992). There are many benefits to using this 3D Petri Dish® system. There is no need for cells to form unnatural adhesions or to add attachment

factors, extracellular matrix, or scaffolding. It allows for cell-cell interactions and communication that would occur in normal tissue. It also allows for normal cell density and the cells can be in contact with media on all sides. The 3D molds are also in an ordered array which makes for easy imaging. There is also no need for any enzymatic treatments to remove cells from the wells. These spheroids can be used for a lot of techniques such as RT-PCR, Western blots, transplantation, immune-staining, and histology (Dean et al. 2007).

Ciona intestinalis as a Model Organism

Ciona intestinalis is a solitary ascidian and being part of the Urochordata is the closest invertebrate group to the vertebrates phylogenetically (Corbo, Di Gregorio, and Levine 2001). *C. intestinalis* is an invasive species to the marine environment of Rhode Island, and is readily available for collection between the months of May and December. *C. intestinalis* was also one of the first animals to have its genome fully sequenced. It has recently been shown that there are two sub-species of *C. intestinalis*, species A and species B. Species A, now called *Ciona robusta*, is found on the west coast of North America and its genome has been extensively annotated. Species B, now called *C. intestinalis*, is found on the east coast of North America, and is found in the waters of Rhode Island. This species has a less well annotated genome.

C. intestinalis develop very rapidly, reaching the larval stage within 24 hours of fertilization. The life cycle of *C. intestinalis*, like most marine invertebrates, begins with fertilization after which the zygote undergoes embryogenesis, hatches from the

chorion (eggshell) as a swimming larva, the larva settles and then undergoes metamorphosis into a juvenile which grows and develops into a reproductively competent adult, thus beginning the cycle again. The complete life cycle from egg to mature, reproductively competent adult takes about 3 months. This is ideal for developmental and genetic studies as the life cycle is so fast (Corbo, Di Gregorio, and Levine 2001). *C. intestinalis* has a relatively small genome size, the haploid genome only contains about 1/20th of the number of base pairs as the human genome (Simmen et al. 1998). It has been found that many of these genes, especially the ones expressed during the larval stage, have molecular homologies with the genes expressed during development in vertebrates (Takahashi et al. 1999). All together this makes *Ciona intestinalis* a good model organism.

C. intestinalis Ovarian Development

Ascidians are hermaphroditic animals, meaning they have both male and female gonads. The gonads sit in a loop of the intestine within a sac that also contains the heart and is constantly bathed in hemolymph. Development of the germ cells in solitary ascidians during embryologic development is isolated to several cells in the endodermal strand that can be seen during tailbud stage (Fujimura and Takamura 2000). In juvenile *C. intestinalis*, the gonad rudiment is connected to the dorsal strand and originates from a portion of the tadpole stage tail that is resorbed during the settling and metamorphosis process (Takamura, Fujimura, and Yamaguchi 2002; Yamamoto and Okada 1999).

During metamorphosis, the larval tail is resorbed and a mass of tissue from the resorbed tail is the origin of the gonad. The gonad rudiment can be seen using light microscopy as early as 2-3 days post metamorphosis in juvenile *C. intestinalis*. Electron microscopic examination of the early gonad rudiment shows initiation of germ cell formation around blood cells and phagocytic cells that had engulfed the cellular debris of the resorbed tadpole tail. As the 2-day juvenile develops, the phagocytic cells become more infrequent, and more germ cells are found in the area. Somatic cells can begin to be found along with the germ cells in the 3-day old juvenile. By day 4-5, germ cells become an independent structure from the phagocytic cells called the gonad rudiment. As the juvenile develops, the number of germ cells and somatic cells continues to increase when on day 7 a cavity begins to develop in the gonad rudiment. The cavity continues to enlarge from day 8 to day 10 post metamorphosis with the majority of germ and somatic cells underneath the empty cavity (Yamamoto and Okada 1999).

The gonad rudiment begins to differentiate into both the ovaries and testes about 11-12 days after metamorphosis. A rounded vesicle of germ cells containing a cavity lined by somatic cells begins to bud off of the gonad rudiment to become the testis and the remainder of the rudiment containing somatic cells associated with each germ cell becomes the ovary. By day 12, the new testicular rudiment completely separates from the ovary rudiment and migrates towards the intestine while the ovary rudiment begins to form lobules and the beginning of the oviduct begins to extend towards the atrial siphon. By day 13-14, the testicular rudiment becomes

branched with small follicles at the end of each branch and the ovarian rudiment lobules branched and attached to one another. By day 15-16, the testicular rudiment becomes more club shaped and the sperm duct extends parallel to the oviduct towards the atrial siphon. The ovarian rudiment moves into the ventral loop of the intestine by day 18 (Okada and Yamamoto 1999).

In the ovary, oocytes develop surrounded by an acellular vitelline coat and between the oocyte and the vitelline coat (the perivitelline space) there are test cells. The vitelline coat is surrounded by follicle cells that produce substances to attract sperm to the oocyte (Noriyuki Satoh 1994). As oocyte maturation continues, the follicle cells extend away from the oocyte within the chorion forming a starburst like shape to the chorion. Once the oocyte moves from the ovary, into the follicle stalk, it moves to the oviduct and continues to mature until it is released from the oviduct into the surrounding water (Okada and Yamamoto 1993).

1.2 Methods and Materials

Biological Materials

Gravid *C. intestinalis* adults were collected from Point Judith Marina in South Kingstown, Rhode Island between May and October with a small hiatus during August when the water is at its hottest. Animals were placed in an aquarium under constant light for 36 to 48 hours after collection to allow for the animals to store gametes.

Ovarian Tissue Preparation

The ovary was dissected and rinsed in 75% ethanol for 5 seconds to remove any protists that may have been commensal in the animal. Ovaries were then cut into

approximately 1 cubic millimeter pieces. Cell dissociation was performed by placing ovary fragments in a 0.01% trypsin solution in filtered sea water (FSW) for 15-20 minutes. (FSW was made from seawater collected in Narragansett Bay, RI and filtered using 0.22 μm bottle filters.) The tissue was triturated every few minutes to completely dissociate the ovarian cells. Cells were transferred to a 2mL tube and spun down at 800 rpm for 3 minutes, the supernatant was discarded, new filtered sea water was added, cells were resuspended, and the washing process was repeated 3 times. After the final wash, cells were resuspended in culture medium and 75μl of the cell media mixture was seeded into each agarose castings and the cells were allowed to settle into the wells for 15 minutes before the additional 1mL of media was added to each well. Media was changed weekly and all tissue preparation and media changes were done under sterile conditions.

3D Petri Dish® System

The 3D Petri Dish® system (Microtissues, Inc.) was used to create microwells for the tissue culture. 800μm diameter x 800μm depth well (24-35 large spheroid) and 400μm diameter x 800μm depth well (24-96 small spheroid) molds were filled with 2% agarose in FSW. Once cooled, the agarose was removed from the molds and transferred to 24 well plates (Figure 1). Prior to seeding the cells, the agarose microwells were allowed to equilibrate in media solution for 24 hours (Napolitano et al. 2007; Dean et al. 2007; Achilli, Meyer, and Morgan 2012).

3D Petri Dish® vs Culture Treated Plastic

C. intestinalis ovarian tissue was prepared as described above. Cells were counted on a hemocytometer prior to seeding so as to track the growth from time point zero (the day the cells were seeded). Ovarian cells were seeded in both the agarose casting and on culture treated plastic (CytoOne CC7672-7524). In two separate trials, on days 7, 14, and 22 of growth in culture, 8 samples of each system were collected for cell counting to estimate the cell growth and proliferation. In the agarose casting the cells were collected by simple by trituration. Because the cells made no adhesions to the agarose they were easily suspended in the media and dissociated using the force of the pipettor. On the culture treated plastic, 0.01% trypsin was added to culture media and allowed to sit for 1 minutes. The media was then agitated by trituration until the cells were no longer adherent to the culture treated plastic. Tissue on culture treated plastic as well as in agarose castings was triturated with 1mL of media and cells were counted using a hemocytometer. This study was done using Powdered Leibowitz's L-15 Medium (Gibco 41300-039) made with filtered seawater containing 5% fetal bovine serum (FBS) (Gibco 16000-036), 50 U Penicillin/50 μg Streptomycin per ml (Gibco 15070-063), Antibiotic-Antimycotic: 10 U penicillin, 10 μg streptomycin, .025 μg Gibco Amphotericin B per ml (Gibco 15240-062), and 2mM L- Glutamine (Gibco 25030-081).

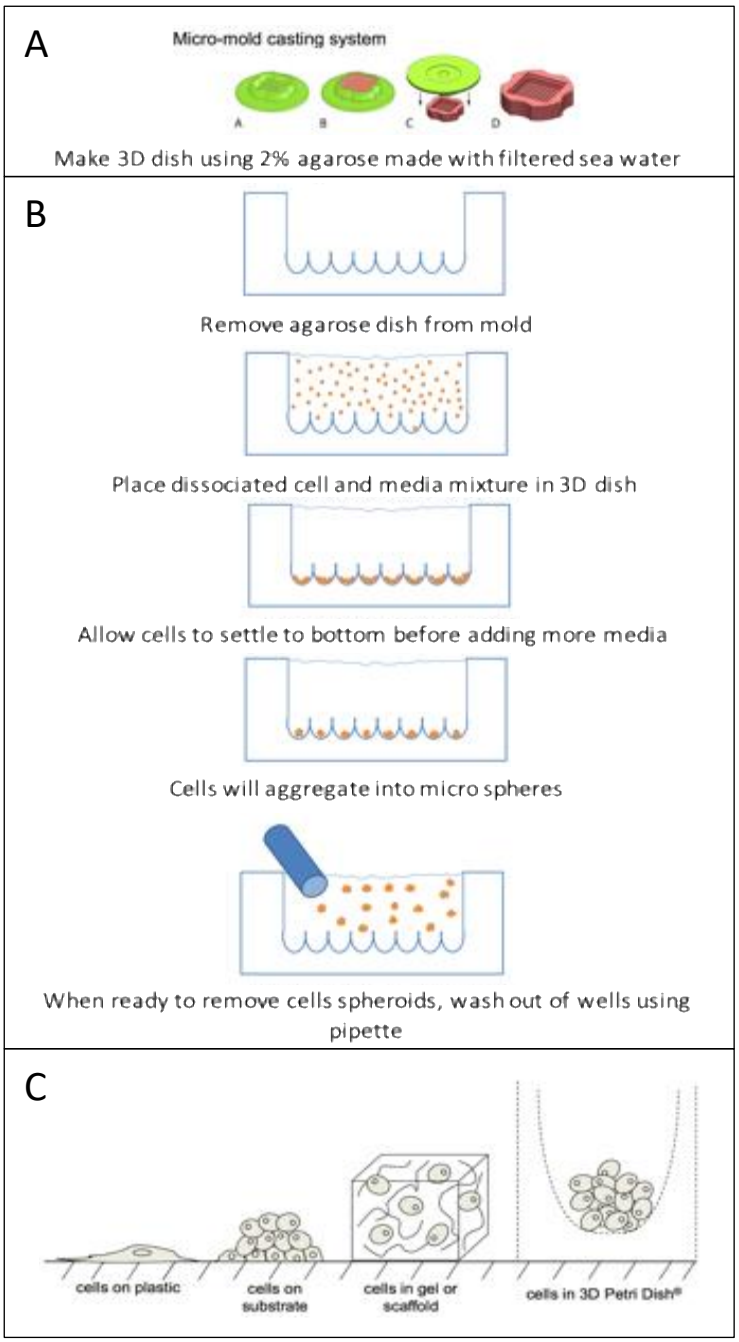

Figure 1: Methods for making agarose castings in 3D Petri Dish system (A), seeding and spheroid collection from agarose castings (B) and comparison of 3D Petri Dish culture system compared to other culture systems (C) (modified from Microtissues Inc.)

Culture Media Formulation

Powdered Leibowitz's L-15 Medium (Gibco 41300-039) was reconstituted in either 100% FSW or 50% FSW. Various concentrations of either fetal bovine serum (FBS) or *C. intestinalis* hemolymph were added (see results). Hemolymph was collected via direct heart puncture. Collected hemolymph from multiple animals was pooled, frozen to kill any protist or commensal bacteria that live in the bloodstream of the animals, and then filter sterilized (0.2μm filter) before added to culture medium. After filtration, if hemolymph was not added to the media right away it was stored at -20°C. All media solutions contained 50 U Penicillin/50 μg Streptomycin per ml (Gibco 15070-063), Antibiotic-Antimycotic: 10 U penicillin, 10 μg streptomycin, .025 μg Gibco Amphotericin B per ml (Gibco 15240-062), and 2mM L-Glutamine (Gibco 25030-081).

Ovarian Tissue Culture Over Time

Ciona intestinalis ovarian tissue culture grown with culture media made of 50% FSW containing 5% hemolymph, 50 U Penicillin/50 μg Streptomycin per ml (Gibco 15070-063), Antibiotic-Antimycotic: 10 U penicillin, 10 μg streptomycin, .025 μg Gibco Amphotericin B per ml (Gibco 15240-062), and 2mM L-Glutamine (Gibco 25030-081). Agarose casting was marked in one corner to ensure that images were taken of the same 9 wells over 7 days in culture. Images were taken on an inverted microscope so as to not contaminate the culture.

Histological Preparation

The entire agarose casting containing *C. intestinalis* ovarian cell culture were fixed in 10% formalin in PBS overnight. The next day, fixed cultures were rinsed in PBS for 2 hours, and dehydrated in 50% ethanol for 1 hour then 70% ethanol overnight. Fixed cultures were then dehydrated in increasing concentrations of tertbutyl alcohol (20%, 35%, 55%, 75%, 100%, 100%) then imbedded in paraffin wax. The paraffin wax is then forced into the tissue by placing the molten wax containing cultures into a vacuum oven. The cultures were then added to a mold and covered in fresh paraffin wax and allowed to cool. Once cooled, the cultures were then sliced into 8(μm) slices on a microtome (American Optical Company Spencer "820" Microtome). Slices were then mounted onto subbed slides. To stain using hematoxylin and eosin, slides were deparaffinized by submerging them in xylene twice for 3 minutes each, rehydrated in washes of decreasing ethanol concentrations (100%, 95%, 70%, tap water) for 3 minutes per wash, stained with hematoxylin for 10 minutes, washed in tap water to activate hematoxylin for 3 minutes, stained in 25% eosin in 70% ethanol for 10 seconds, dehydrated once more in increasing concentrations of ethanol (70%, 95%, 100%, 100%) for 3 minutes each, deparaffinized by submerging in xylene twice more for 3 minutes each and had a coverslip permanently mounted(Corliss and Humason 1974). To stain using Toludine Blue (Sigma C.I. 52040) according to the manufactures protocol, slides were deparaffinized and rehydrated, stained with 0.01% Toludine Blue in water for 1

minute, washed in distilled water for 1 minute, dehydrated once more and had a coverslip permanently mounted.

Live Dead Assay

Hoechst 33342 and Propidium iodide (PI) were used to stain aggregations to determine the ratio of live to dead cells found within the cultures. As a killed control for cell death, cells were incubated with 10% EtOH for 10 minutes prior to addition of stains. The media was changed in the agarose castings containing *C. intestinalis* ovarian cell culture 10 minutes prior to staining in order to remove any floating or non-adherent debris. Hoechst 33342 and Propidium iodide (PI) were added to the media, each at a final concentration of 1μg/ml. After 1 hour incubation with fluorescent stains the cultures were washed with fresh media to remove any stain not bound within the cells (Lema, Varela-Ramirez, and Aguilera 2011). Cell cultures were then fixed in 2% paraformaldehyde in Ca/Mg-free seawater for 30 minutes. Cultures were washed 4 times in phosphate buffered saline (PBS) with 0.1% Tween-20 (P-Tween) and then washed twice in PBS for 15 minutes. Cultures were stored in PBS at 4°C until ready to be imaged. Hoechst 33342 will penetrate the cell membrane of both live and dead cells and fluoresce blue. Propidium iodide will only penetrate the cell membrane of dead cells and produce red fluorescence (Lema, Varela-Ramirez, and Aguilera 2011).

1.3 Results

3D Petri Dish® vs Culture Treated Plastic

I first compared whether there was more cell growth and proliferation in the agarose microwells as opposed to the traditional culture treated plastic that is commonly used in cell culture techniques (Figure 2). Day zero (the day the cells were seeded into each system) started with an average of 125 cells/µl on the culture treated plastic and 130 cells/µl in the agarose casting. There was no statistical difference between the number of cells seeded in agarose castings versus culture treated plastic. Cells proliferated significantly faster in the agarose castings than those on culture treated plastic for all 3 subsequent time points. By day 7, cell counts in the agarose castings were about three times higher than on the culture treated plastic, which had declined slightly. By day 14, cell counts in the agarose castings, which had increased slightly, remained about three times higher than on the culture treated plastic, which had also increased slightly. By day 22, cell counts in the agarose castings, which had increased slightly, were about twice that of the culture treated plastic, which had also increased slightly.

Culture Media Trials

I next tested what types of growth additives and at what concentration yielded the most cell proliferation. I found that cells grew significantly better in media made with a base of L-15 media in 50% filtered seawater with a 5% (v/v) growth additive of *C. intestinalis* hemolymph (Figure 3). Cells were seeded into the agarose casting wells at a concentration of 22 cells/µl for all media formulations that

were tested. At day 5 all cells counts had increased, with L-15 media made with 50% FSW media containing hemolymph having the highest counts, but there was no statistical difference between any of the media formulations.

By day 13, cell proliferation was fastest in cultures containing L-15 media made with 50% FSW containing 5% *Ciona* hemolymph. The cell counts in the L-15

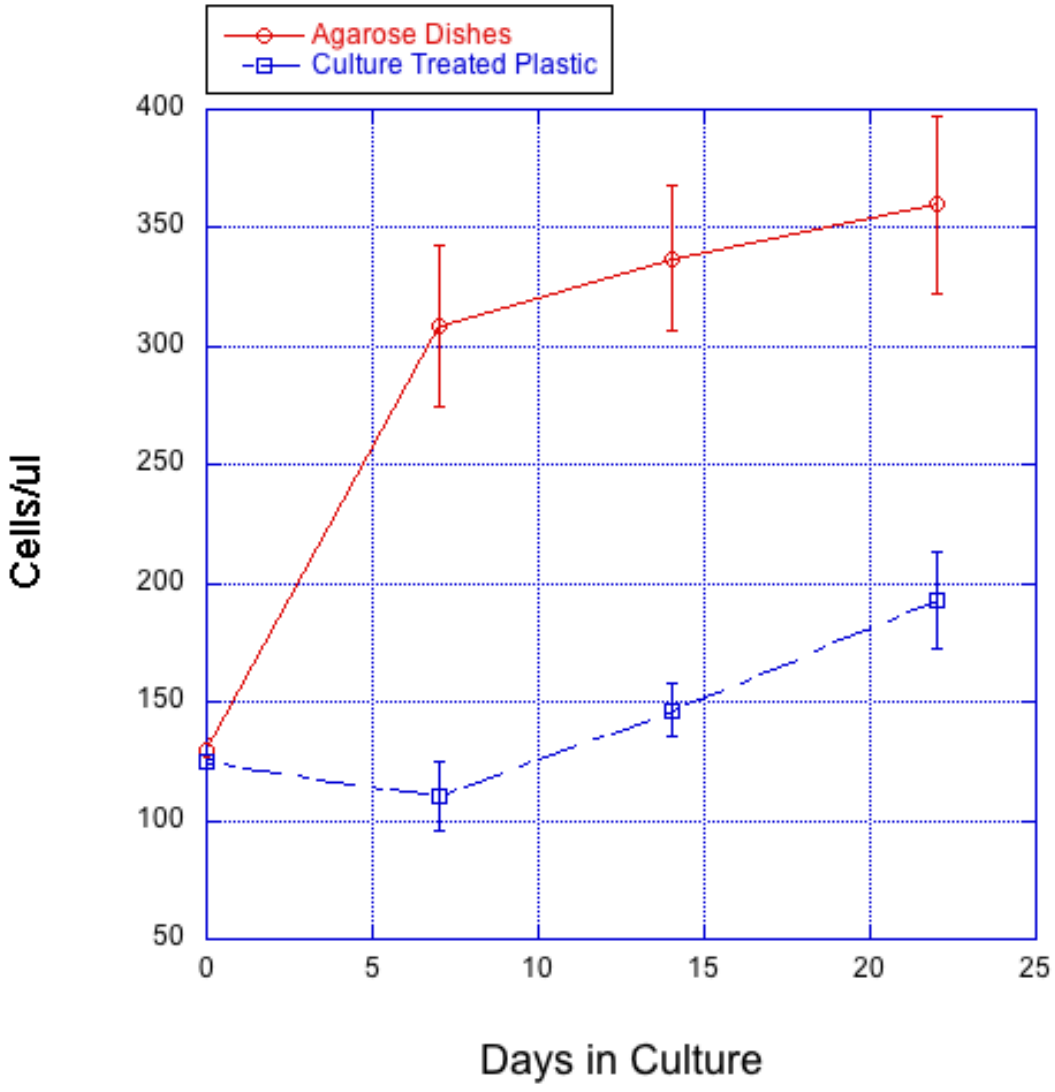

Figure 2: *Ciona intesintalis* ovarian cell growth and proliferation over 22 days in culture on culture treated plastic (blue) or in agarose castings (red). Maximum cell growth and poliferation occurred in the agarose castings. Cell counts are an average of 2 technical repilcates of 4 biological replicates.

media made with 50% FSW containing 5% *Ciona* hemolymph had doubled from day 5. The cell counts were significantly higher than the counts in cultures containing L-15 media made with 50% FSW media containing 5% FBS (P-value 0.0414), the L-15 media made with 100% FSW media containing 5% FBS (P-value 0.0101), the L-15 media made with 100% FSW media containing 5% hemolymph (P-value 0.0093), and the L-15 media made with 100% FSW media containing 10% hemolymph (P-value 0.0171).

By day 20, cell proliferation remained highest in in cultures containing L-15 media made with 50% FSW containing 5% *Ciona* hemolymph. The counts were significantly higher than the counts in cultures containing L-15 media made with 50% FSW media containing 5% FBS was 36 cells/µl (P-value 0.0258) as the cell counts in this media had declined. The counts for all media formulations increased between day 13 and day 20 with the exception of the L-15 media made with 50% FSW containing 5% FBS, which declined.

Ovarian Tissue Culture Over Time

Figure 4 shows images of the same 9 wells of *C. intestinalis* tissue culture in an agarose casting over 7 days in culture (800µm diameter x 800µm height). Figure 5 shows images of the same well of *C. intestinalis* tissue culture on culture treated plastic over 7 days in culture. Day 0 shows cells that are not associated with one another as they had just been seeded into the culture system that day. As time moves on, the cells become more closely associated with one another and the size of the aggregations increases through Day 7.

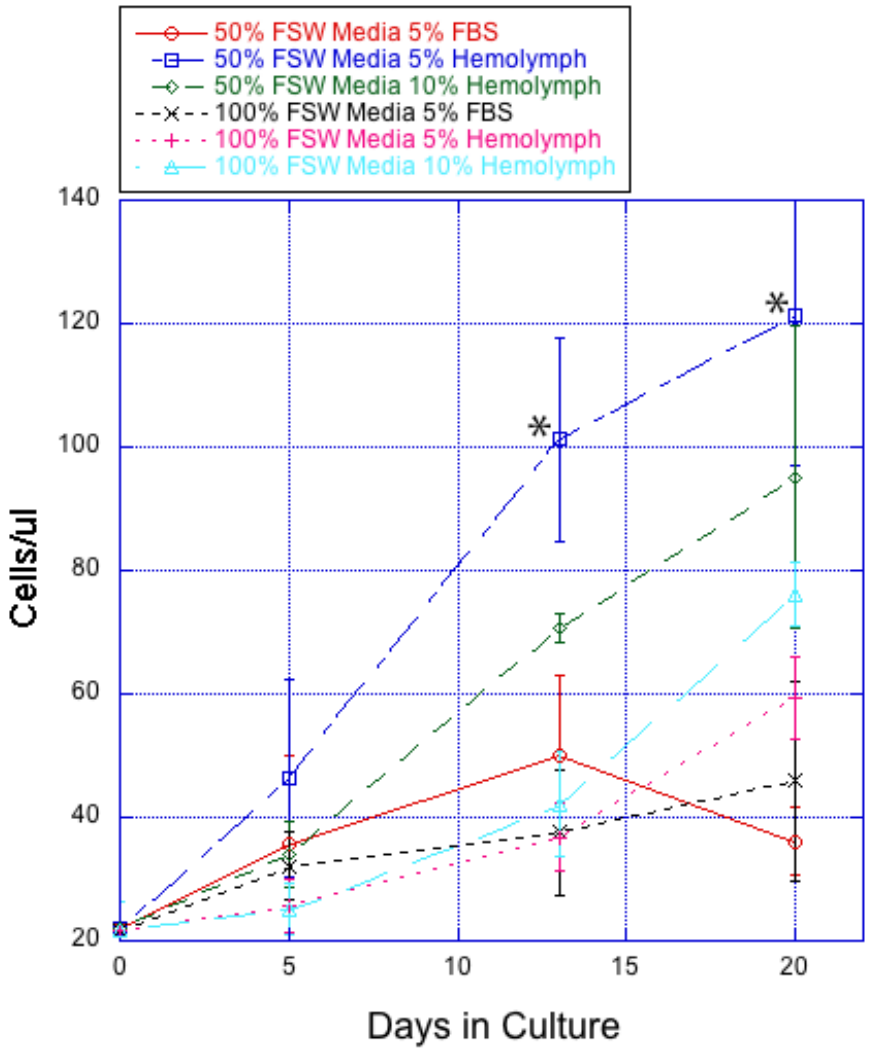

Figure 3: *Ciona intesintalis* ovarian cell growth and proliferation with different culture media formulations over 20 days in culture in agarose castings. All preps made with L-15 medium. Maximum cell growth and proliferation occurred with culture media made with 50% FSW containing 5% *Ciona intestinalis* hemolymph (dark blue squares). Cell counts are an average of 2 technical replicates of 3 biological replicates.

Morphology of Aggregations

Histology of invertebrate tissues in culture, especially marine invertebrate tissues, is very limited. In order to examine if the aggregations forming in the agarose castings were organizing into ovary-like tissue, I compared the histology of intact *C.*

intestinalis ovaries to the histology of the aggregations in culture. Ovarian tissue was stained with either toluidine blue or hematoxylin and eosin (Figure 6). The largest cells are the developing oocyte which will look different depending on which stage of maturation they are in. Directly surrounding the oocyte are the test cells (arrow A). The test cells are held to the oocyte by the vitelline coat (arrow B). Surrounding the vitelline coat are the inner follicular cells (arrow C) followed by the outer follicular cells (arrow D). Once the oocyte is matured enough to leave the ovary, it will flow out the follicle stalk (arrow E) in order to move into the oviduct.

The morphology of the tissue culture over time showed the dissociated cells aggregated together into aggregations that resembled different regions of *C. intestinalis* ovary histology (Figure 7). On day 1 of culture, the ovarian cells came together slightly but as they had only had 24 hours in culture, they did not show a lot of aggregation. By day 3, small groups of cells began to aggregate together forming the beginning of multiple aggregations per well in the agarose casting (white arrow). By day 7, similar to the results of the cell count, there were more cells present as well as growth of the aggregations that were seen in day 3 cultures. By day 14, the aggregations were continuing to grow and show more signs of organization with tissue similar in morphology to the vitelline coat (white arrow) beginning to surround some of the aggregations (Figure 8). By day 21, it appeared that multiple aggregations were beginning to fuse in an attempt to generate a fewer number of larger aggregations within the wells of the agarose casting.

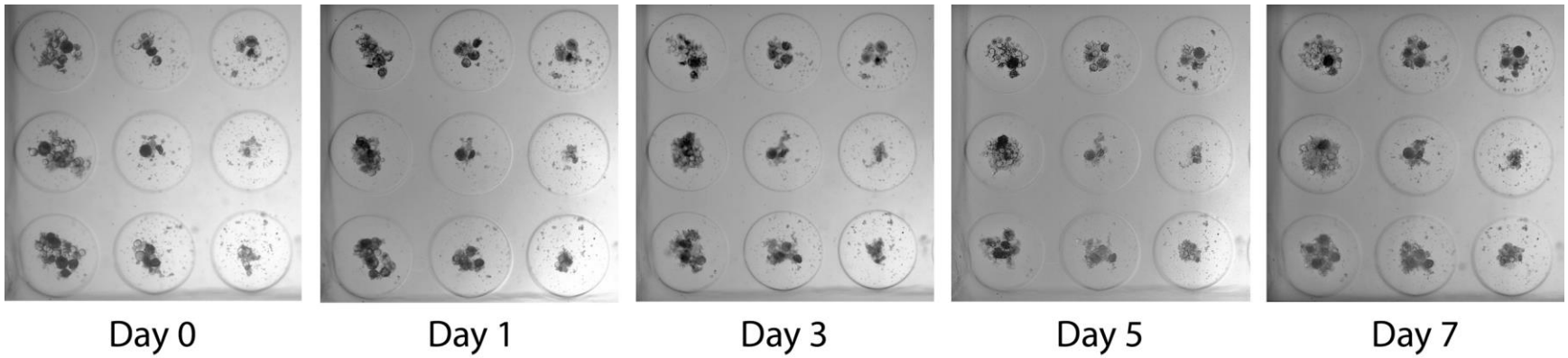

Figure 4: *C. intestinalis* ovarian tissue culture in agarose castings over 7 days in culture. Images were taken using an inverted scope and all images are of the same 9 wells in an agarose casting.

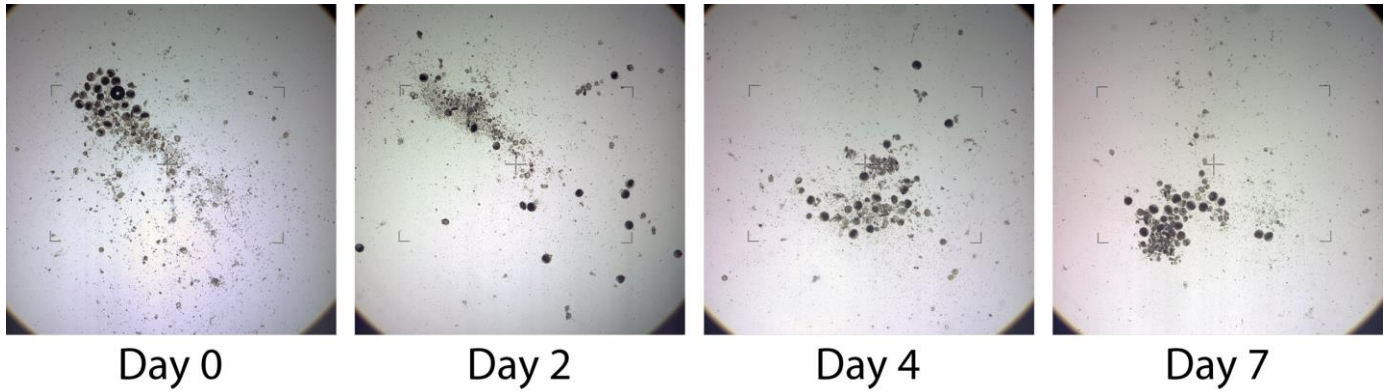

Figure 5: *Ciona intestinalis* ovarian cell growth on culture treated plastic over 7 days

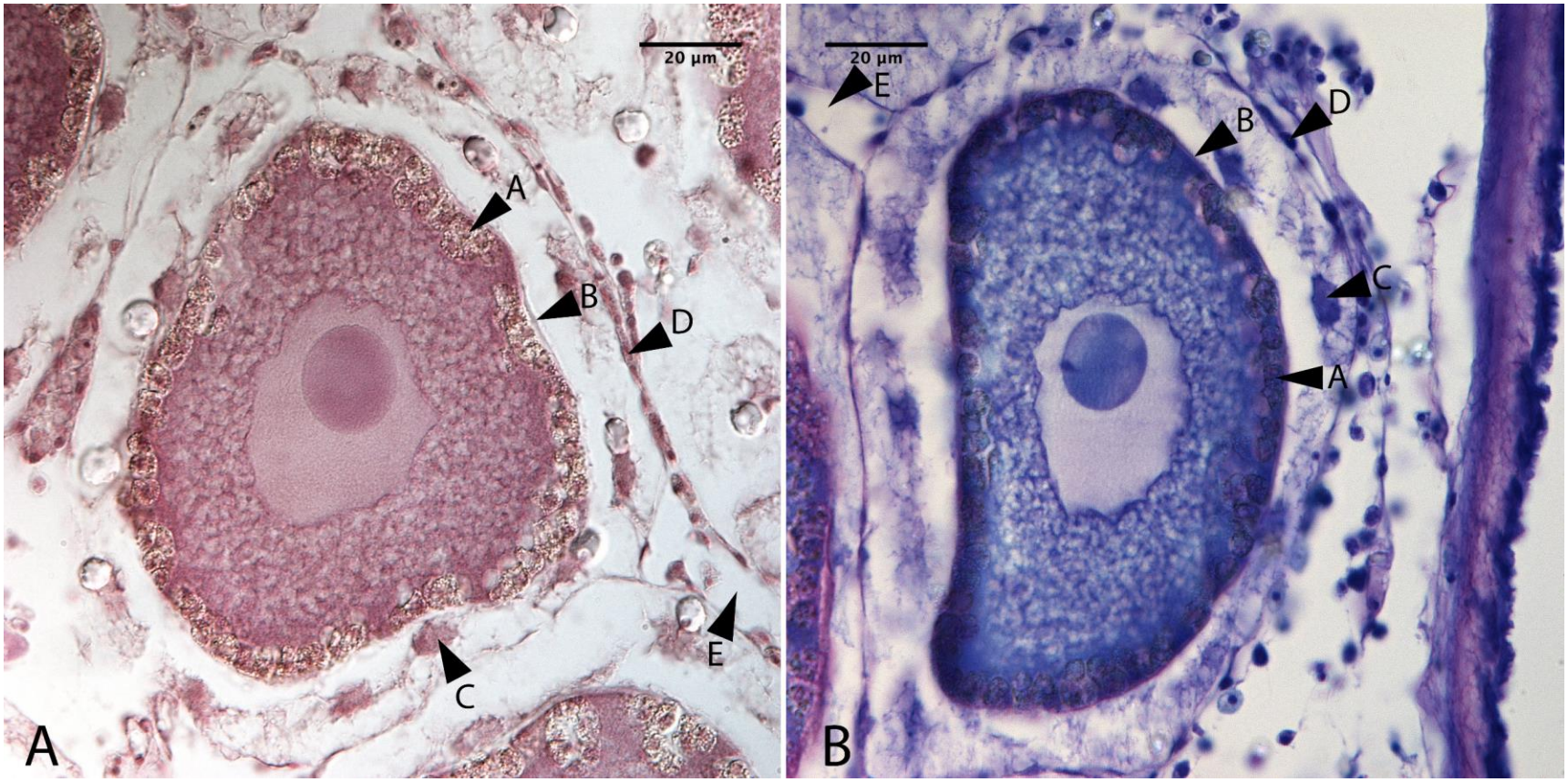

Figure 6: *Ciona intestinalis* whole ovary histology stained with hematoxylin and eosin (A) or toluidine blue (B). Test cells are identified by arrow A. Vitelline coat is identified by arrow B. Inner follicular cells are identified by arrow C. Outer follicular cells are in identified by arrow D. Follicle stalk is identified by arrow E.

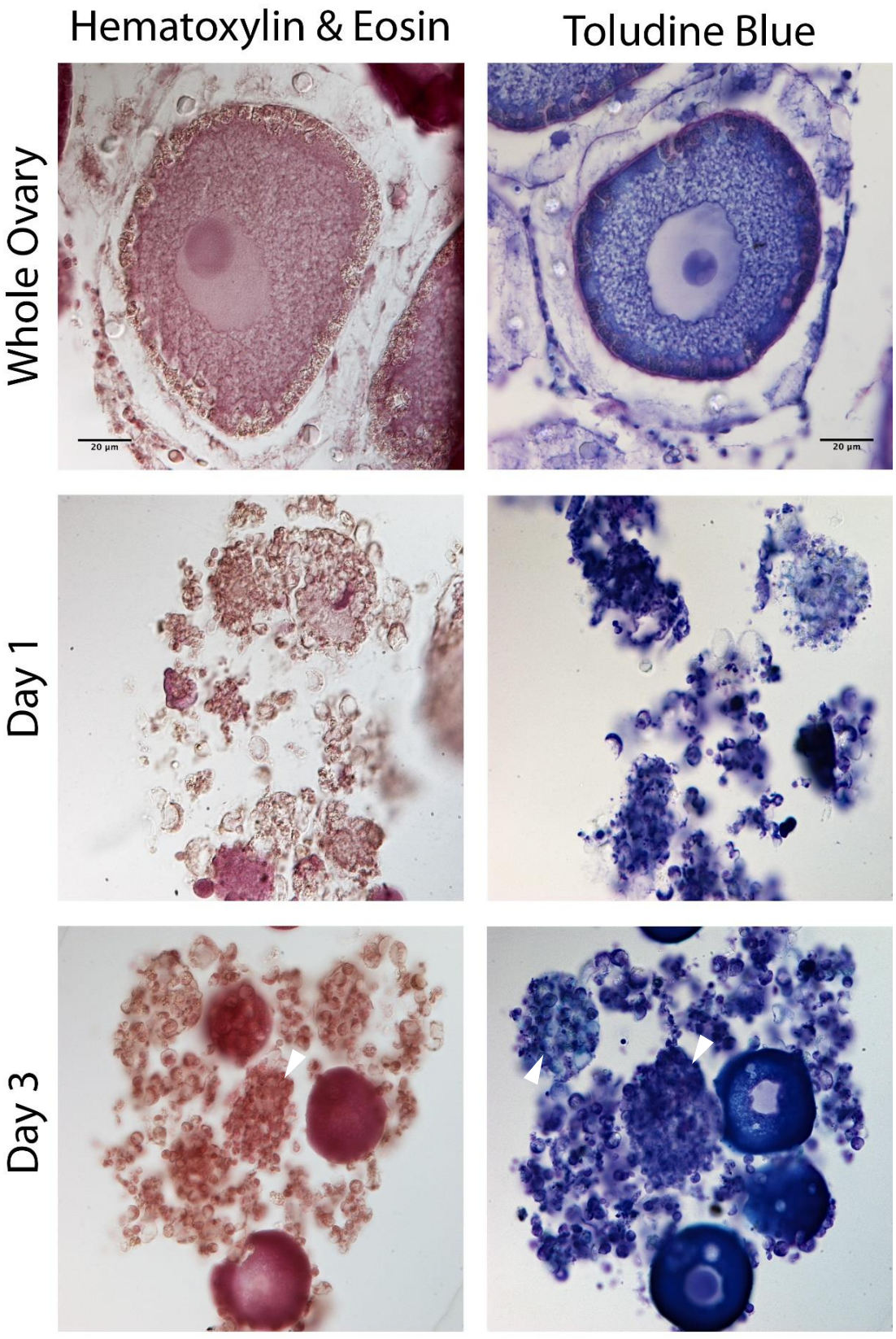
Hematoxylin & Eosin
Toludine Blue
Whole Ovary
Day 1
Day 3
20 µm
20 µm

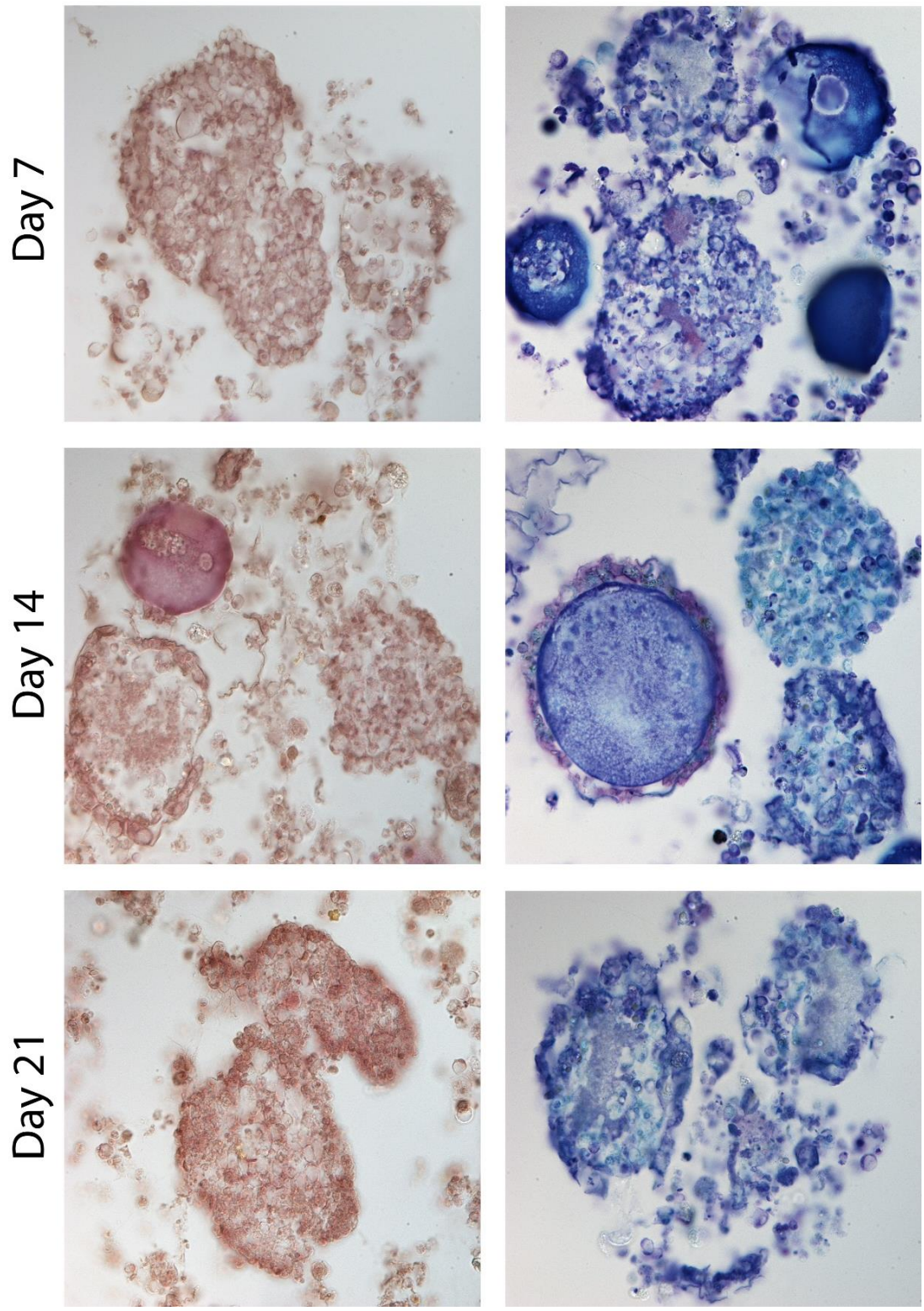

Figure 7: *C. intestinalis* whole ovary histology compared to ovarian tissue aggregation histology over 21 days in culture stained with either hematoxylin and eosin or toluidine blue.

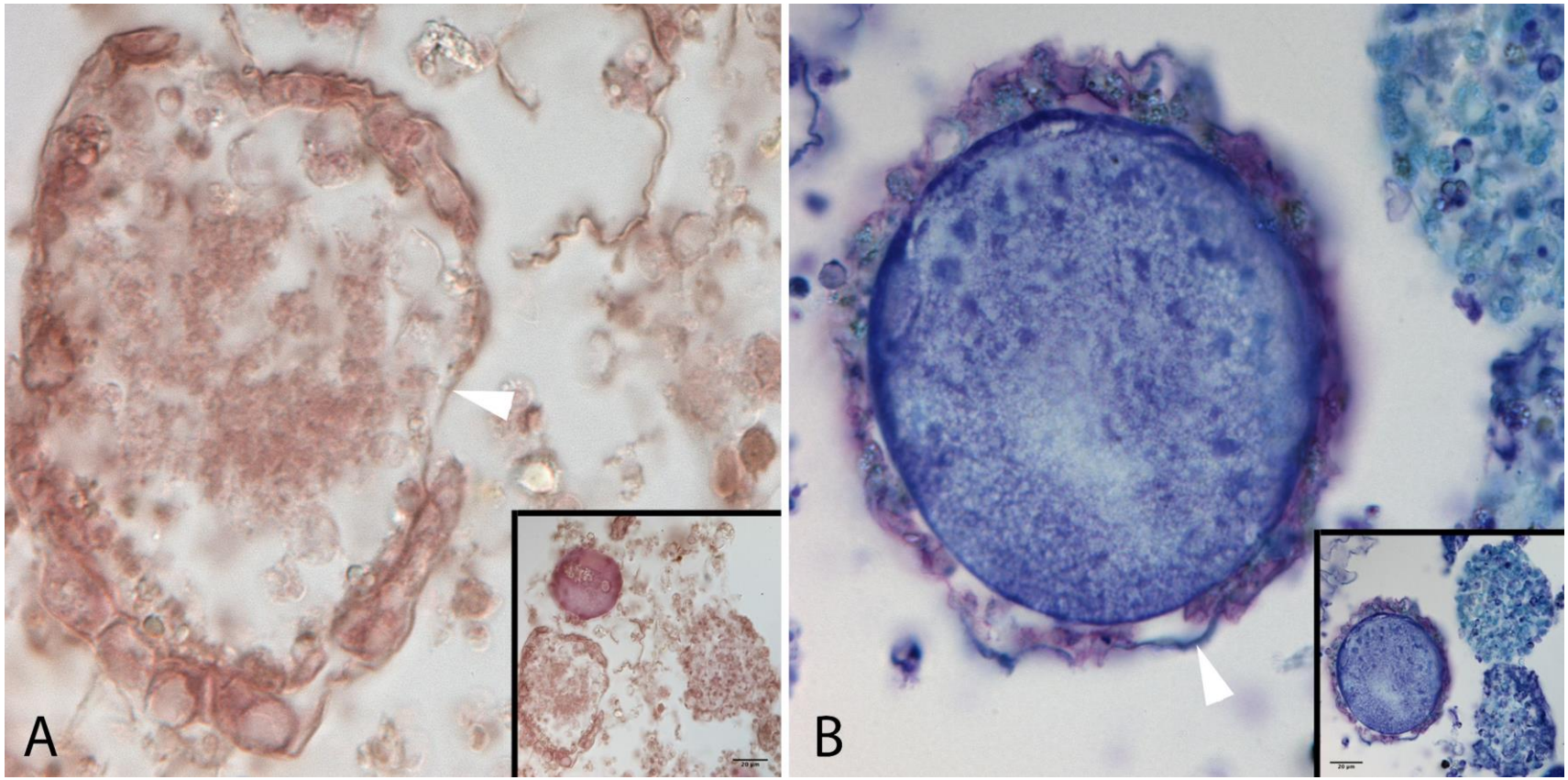

Figure 8: *C. intestinalis* ovarian tissue aggregations in agarose castings after 14 days in culture stained with A: hematoxylin and eosin and B: toluidine blue. White arrow indicates vitelline coat structure around aggregation.

Live Dead Assay

I next checked the viability of the cultured cells with a live dead assay. The assay was conducted on *Ciona intestinalis* ovarian tissue grown in culture for 19 days with L-15 media in 50% FSW containing 5% *Ciona* hemolymph. To remove aggregation from the agarose castings without disrupting the structure of the aggregations, the 3D dishes were inverted onto a microscope slide that had been silanized (RainX). To ensure the aggregations could fall from the recesses in which they were growing, PBS was added to the indentations until there were no more air bubbles seen. A slight lift in one side of the 3D dish while not allowing air in would allow for the aggregations to fall from the recesses within the 3D dish onto the slide. The aggregations were held in place on the slide by small pieces of coverslip glass that had been glued to either side of the slide to prevent the movement of the fluid containing the aggregations off the slide. The aggregations, once removed from the wells, were fragile but held together and can be seen in Figure 9, A & C. When subjected to Hoeschst and PI, microwell aggregations exhibited few dead cells as shown in Figure 9 D (red cells). In the control samples, which were killed by ethanol poisoning, there are many more dead cells as seen in Figure 9 B (red cells).

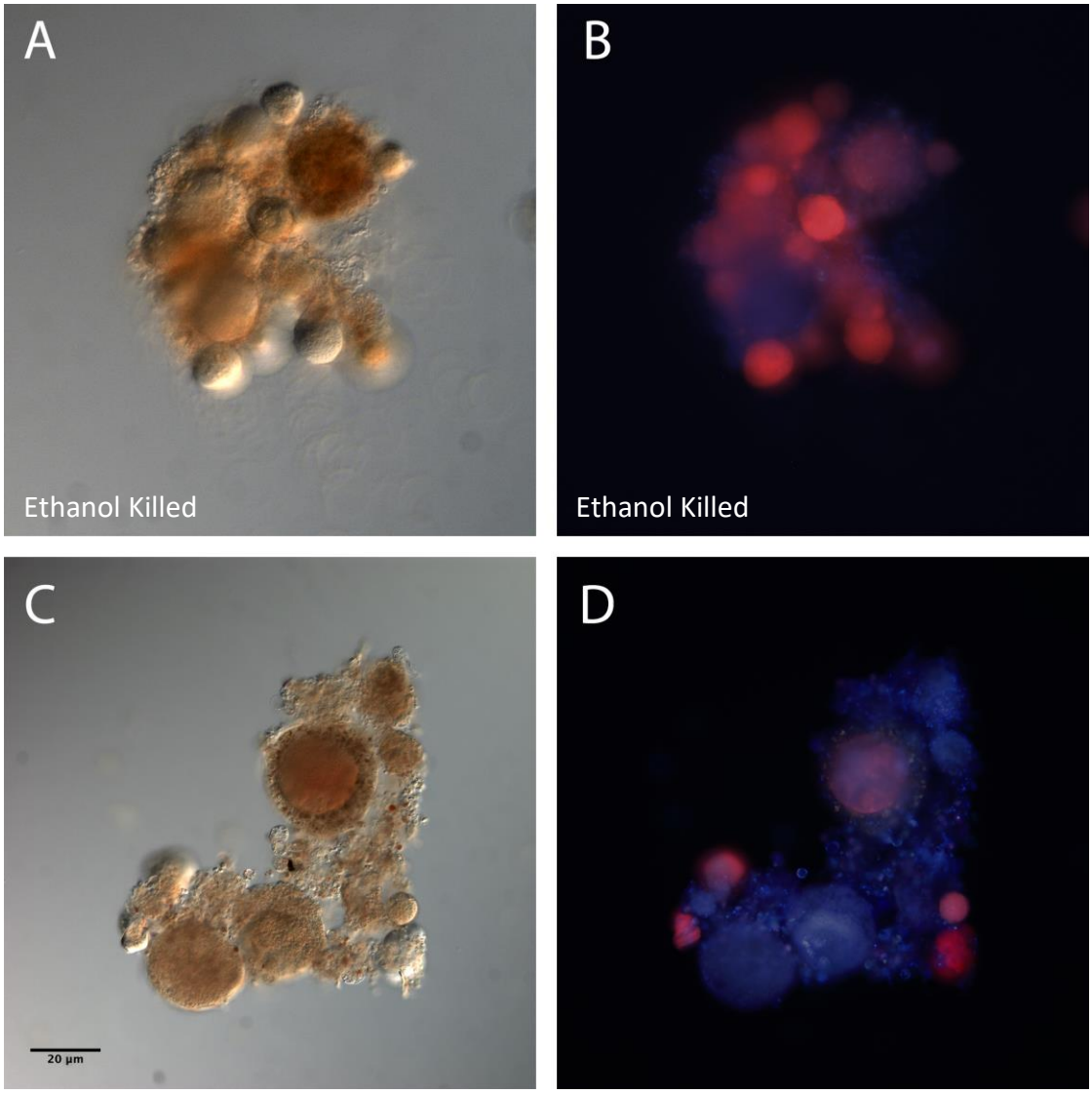

Figure 9: *Ciona intestinalis* ovarian tissue culture hoeschst/propidium iondide stain removed from agarose castings after 19 days of growth. A&B: EtOH killed control *C. intestinalis* ovarian tissue aggregation; C&D: C. intestinalis ovarian tissue aggregations (A&C: brightfield image B&D: fluorescent image of hoeschst (blue; living) and propidium iodide (red; dead))

1.4 Discussion

3D Petri Dish® vs Culture Treated Plastic

When cells are grown on culture treated plastic, they do not associate with each other (Figure 5). The cells will become less 3 dimensional as they flatten out in an attempt to form attachments to the plastic. The agarose casting system allows for the cells to remain in a more natural morphology as they do not form adhesions to the substrate. The agarose casting also potentially allows for better cell-cell interactions because of its 3-dimensionality (Achilli, Meyer, and Morgan 2012; Napolitano et al. 2007; Dean et al. 2007). This increase in cell interactions could allow for the cells to organize properly according to cell type and form an aggregation, as seen in the data in this study. The formation of an aggregation of cells also allows for the removal of the intact aggregation containing multiple cells for use in biochemical assays and physiological experiments.

Culture Media Trials

Optimization of cell culture media was key to optimization of ovarian cell growth in the 3D culture system. Leibovitz's L-15 medium was used as the base media of choice for growth of ovarian tissue culture. Media was purchased in powdered form in order to more closely control the final formulation. Because *C. intestinalis* is a marine organism, its internal organs are likely hypotonic with seawater, and proper osmolarity is needed for optimal cell proliferation. To test this, I used two concentrations of seawater to dissolve the L-15 media, one at 100% and one diluted to 50% with deionized water. All media solutions had 2mM L-Glutamine,

an antimicrobial, and an antibiotic additive (see Materials and Methods). The antibiotics helped to control any potential contamination and the glutamine helps with cell growth and proliferation.

In traditional mammalian cell culture, fetal bovine serum (FBS) is used as a growth additive. FBS was tested in both forms of media at both a 5% and 10% concentration. *C. intestinalis* hemolymph was also tested as a media supplement. It was collected and used as a supplement in both media types at both a 5% and 10% concentration. Hemolymph was collected from freshly collected animals via a direct heart puncture with a syringe. Prior to addition of hemolymph to media for use in culture, hemolymph was filter sterilized (0.2μm) to ensure that any protists that may be commensal in the animal will not contaminate the culture. The culture media was change weekly under all culture conditions.

Although it was not shown in this study, it seems important to note that during embryonic development the gonad rudiment is seen in close association to blood cells (Yamamoto and Okada 1999). *Ciona intestinalis* blood contains stem cells (3.7-5.8 μm), amoebocytes (6-15.9 μm), signet ring cells (7.6-8.4 μm), morula cells (8.4-8.9 μm), compartment cells (6.4-10.3 μm), and orange cells (8.0-9.5 μm) (Rowley 1981) but all of these should have been removed from the hemolymph when filter sterilized. Although the blood cells are filtered out of the hemolymph, there are likely proteins found within the hemolymph that assist in growth of *Ciona* specific cells. Previous work done to culture *Ciona intestinalis* hemocytes also used plasma, or

what I called hemolymph, as a growth additive to their culture medium (B Rinkevich and Rabinowitz 1993).

The results of this study have shown that the optimal media formulation among those tested for maximal cell proliferation is the l-15 media made with 50% filtered seawater with 5% hemolymph as a growth additive (Figure 4). This is likely that, once all the components of the medium are added, the media is closer to the osmolarity of the ovary in vivo. A media with osmolarity similar to that of the internal organs is better for cell growth and proliferation because, in *Ciona intestinalis*, the gonads are enclosed in a membrane and bathed in hemolymph constantly. *Ciona* can also live in the intertidal zone where the salinity can change on a daily basis. This would require that the internal environment of the animal be regulated closely even in the changing environmental conditions.

Hemolymph is also an important growth additive to the culture media because, as previously stated, the ovaries are constantly bathed in hemolymph in vivo. *Ciona intestinalis* have an innate immune system (Noriyuki Satoh 1994). There is a commensal protist, *Cardiosporidium cionae,* that lives within the heart chamber of *Ciona intestinalis* (Hunter, Paight, and Lane 2020). When collecting hemolymph to use as an additive to the culture media, the hemolymph was collected via direct heart puncture. It is likely that these protists were collected along with the hemolymph sample. The hemolymph was filtered prior to the use in the culture media in order to remove all commensal organisms.

It is also important to note that without the addition of hemolymph to the culture media, the tissue cultures became overrun with protists after day 20. These protists are likely commensal to the *Ciona* and live within the sac that encompasses the gonads and heart. During the initial dissection and dissociation of the ovarian tissue, some of these protists may get transferred to the culture with the cells even though the tissue is washed in ethanol. As there were no living blood cells to act on the protists, it is likely that there is a compound found within the hemolymph that prevents the growth of these contaminating protists.

Ascidians have an innate immune system, and the 3 sites of the immune response are the tunic, the hemocytes, and the digestive system. Phenoloxidase, an enzyme involved in the cytotoxic response, has been found in its inactive form within tunicate hemocytes and becomes activated once released outside of the cell (Franchi and Ballarin 2017). Phenoloxidase activation causes the production of reactive oxygen species which induce oxidative stress on the system. This is how phenoloxidase exerts its cytotoxic activity within ascidians (Ballarin and Cammarata 2016). Research has shown that there are immunity-related genes that are up-regulated in the test cell layer and follicle cells of the developing oocytes in *Ciona intestinalis* ovaries, including *Ciona intestinalis* phenoloxidase genes (Parrinello et al. 2015; 2018). This suggests that some of the ovarian tissue cells themselves could be participating in the control of the protist growth in culture. This also suggests that immune function within *Ciona intestinalis* is upregulated within the ovaries, making

them a good tissue to grow in culture because the tissue would aid in immune regulation of potential contamination.

Ovarian Tissue Culture Over Time

The visible growth of *C. intestinalis* ovarian tissue in the agarose castings was tracked over a 21 day period to assess if the tissue was forming aggregations and if those aggregations were growing over time. As seen in the inverted microscope images in Figure 4, from Day 0 (the day the tissue was seeded in culture) to Day 1 the cells come together more closely. This is the first indication of aggregation of the tissue, although it is not clear as to how this aggregation is occurring. The tissue could be coming together via cell cell interactions or it could be coming together due to the "egg carton" shape of the wells where the bottom of the well has a smaller diameter than the top or some combination of these two causes. The most promising evidence shown in these images is the increase in density of the cultures by Day 7 in culture (Figure 4). This shows that there is cell growth and proliferation in this culture system.

Morphology of Aggregations

If the morphology of the aggregations in the ovarian culture system looks similar to the morphology of the whole ovary tissue, this would suggest that the cells can self-organize into similar structures seen in the ovary. One determinant of the ability of the cells to organize around an oocyte could be the maturation state of the oocyte itself. As the cells were not sorted when the tissue was cultured, there were likely oocytes at multiple states of maturation when seeded into the culture. The less

mature oocytes would be better equipped to communicate with the supporting cells of the ovary as they rely on them for growth and development. More mature oocytes that are ready for movement from the ovary into the follicle stalk would no longer rely on the surrounding cells for maturation. If ovarian tissue cells were seeded with a less mature oocyte, they would likely be able to aggregate around the oocyte while if the oocyte is mature, they likely will not be able to aggregate properly.

It is important to note that the whole ovarian tissue, as depicted in Figure 6, is not a very compact tissue. In fact, when the ovary was dissected out of the *Ciona*, more often than not the tissue would almost fall apart before any trypsin was added. Ovarian tissue as a whole is not expected to be dense as the oocytes require space to develop and grow. Once the oocytes are mature enough, they move through the follicle stalk into the oviduct where they continue to mature until they are released. As can be seen in Figure 7 and Figure 8, the aggregations of ovarian tissue in culture are also not very dense. This is consistent with the morphology seen in the whole ovary tissue.

Live Dead Assay

Results of the live dead assay showed very few dead cells in the *Ciona* ovarian tissue aggregations as compared to the ethanol killed aggregations (Figure 9). This suggests that even after 19 days in culture, the aggregations are still living on the culture media. This also verifies again that the agarose casting system is effective for growth of *C. intesintalis* ovarian tissue culture. Of importance to note was the fragility of the aggregations upon removal from the agarose casting system. Removal

using a pipette to suck up the aggregations from the wells of the agarose casting was damaging to the aggregations. This caused the aggregations to dissociate very easily destroying them. In order to remove the aggregations from the wells without dissociation, I had to invert the agarose casting onto a slide to allow for the aggregations to “fall” out of the wells rather than removing them with a pipettor.

1.5 Conclusions

In this study, I have shown that tissue culture using *Ciona intestinalis* ovarian tissue has increased cell proliferation in the 3D Petri Dish® system grown with L-15 media made in 50% filtered sea water containing 5% *Ciona* hemolymph. Histological comparison of the morphology of whole *Ciona* ovaries to the tissue culture aggregations showed development of similar structures in the tissue culture after 14 days in culture. Live dead analysis of the aggregations showed that *Ciona* ovarian tissue culture aggregations were still living after 19 days in culture.

There are many advantages to generating new tissue culture methods, especially with the lack of marine invertebrate tissue cultures available to on the market. Using tissue aggregations in culture could prove to be very useful in a variety of biochemical, biological, and physiological experiments. Ovarian tissue culture of *Ciona intestinalis* and other marine invertebrates could prove useful to understanding the effects of global climate change and pollutions on invertebrate reproduction. Tissue culture aggregations could be subjected increasing temperature or varying concentrations of pollutants and analyzed for changes in gene expression.

Chapter 2: Shp2 is Required for Normal Embryogenesis in *Ciona intestinalis*

2.1 Introduction

Proteomic Identification of Temperature Stress Proteins

Environmental stress, such as changes in temperature, salinity, or toxins can result in changes in protein expression and function. In a recent review article, proteomic analysis of acute heat stress for 1 hour in two species of blue mussels showed changes in proteins involved in oxidative stress, cytoskeleton remodeling, and signaling (Tomanek 2014). It was also suggested that, in two species of *Ciona*, this acute heat stress causes the breakdown of the cytoskeleton. The comparison of the acute stress response in multiple species of marine invertebrates shows that, along with the need for heat shock proteins, the cytoskeleton is extremely sensitive to and can degrade under heat stress. This comparison also showed that the increase in reactive oxygen species under acute temperature stress leads to an increase in oxidative stress proteins (Tomanek 2014).

Previous work from the Irvine lab used shotgun proteomics to identify differentially regulated proteins in the ovaries of *Ciona intestinalis* reared at a control temperature of 18°C and a stress temperature of 22°C (Irvine et al. 2019). *C. intestinalis* were reared for 120 days at 18°C or 22°C, after which the ovaries were removed and analyzed for protein expression. There were 62 proteins identified as differentially regulated at 22°C as compared to 18°C. Shp2 (PTPN11) was found to be upregulated 114-fold in ovaries of *Ciona* that were reared under high temperature

stress, the highest upregulated protein identified in this study (Lopez et al. 2017) . Shp2 was the major protein of interest that emerged from this study because it was the most upregulated protein at high temperatures.

Shp2 (SH2 domain-containing tyrosine phosphatase 2)

Shp2 (SH2 domain-containing tyrosine phosphatase 2), a protein tyrosine phosphatase (PTP), is encoded by the gene PTPN-11(Lopez et al. 2017). Shp2 is conserved in structure and function from invertebrates through mammals. Protein tyrosine phosphatases (PTPs) are enzymes, of which there are about 90 in humans, that catalyze dephosphorylation events. PTPs that contain two SH2 domains (N-SH2 and C-SH2) as well as a PTP catalytic domain and a C-terminal tail are classified as Shp proteins. Within the PTP catalytic domain there is a motif that contains the key residues for catalysis. The C terminal end of Shp proteins contains regulatory residues. Shp proteins exist in either a closed, auto-inhibited state or in an open, activated state. In the closed, auto-inhibited state, the N-SH2 domain interacts with the catalytic site and physically blocks the catalytic activity of the PTP domain. In the open, activated state, the N-SH2 domain is no longer interacting with the catalytic site, due to the interaction with upstream signaling proteins or the phosphorylated C terminal regulatory residues, to allow for dephosphorylation to occur. There are two Shp proteins found in vertebrates, Shp1 and Shp2, and some proteins can bind to both while others can bind only to one specifically (Neel, Gu, and Pao 2003; Tajan et al. 2015).

Shp2 Function

Shp2 is required for the sustained activation of the Erk/MAP kinase (MapK) pathway in most cells, acts upstream of Ras and FGF, inhibits the Jnk pathway, and activates or inhibits the P13/Akt pathway (Tajan et al. 2015; Neel, Gu, and Pao 2003; Feng 1999). Shp2 interacts with many receptor protein tyrosine kinases (R-PTKs) and the SH2 domain of Shp2 recognizes the phosphotyrosine site on the PTK. When a ligand is bound to the SH2 domain of Shp2, phosphatase activity is increased. The SH2 domain also facilitates the association of enzymes with their substrates (Feng 1999). Thus, Shp2 acts as both an adaptor protein as well as an enzyme. Shp2 has also been shown to play a role in cytokine signaling, cell adhesion, cell migration, cytoskeletal remodeling, cell proliferation, stem-cell renewal, and cell differentiation (Feng 1999; Hale and den Hertog 2017).

The proposed mechanism of Shp2 function is described as follows: A ligand binds to a R-PTK which recruits Shp2 and Shp2 is activated. Activated Shp2 then transduces the signal to the nucleus through downstream target activation. Activated Shp2 also interacts with other transmembrane proteins to transduce the signal to neighboring cells. This allows for the signal to be received by one cell and propagated to many closely associated surrounding cells. This mechanism during a sensitive process, such as development, must be coordinated precisely (Feng 1999). Incorrect function of Shp2 could lead to a host of problems.

Mutations in the PTPN11 gene in humans are associated with Noonan syndrome (NS), Noonan syndrome with multiple lentigines (NSML), and many types

of malignancies (Romano et al. 2010; Lorca et al. 2020; Chen et al. 2006; Tajan et al. 2015; Orrego-González, Martin-Restrepo, and Velez-Van-Meerbeke 2021). Noonan syndrome is an autosomal dominant disorder and occurs in 1 in 1,000-2,500 births. It is characterized by craniofacial abnormalities, chest deformities, short stature, and congenital heart disease. Mutations in the PTPN11 gene, that encodes for the Shp2 protein, was first identified as the genetic cause for NS in 2001 (Romano et al. 2010). The mutations found in Shp2 in Noonan syndrome are gain of function mutations (Orrego-González, Martin-Restrepo, and Velez-Van-Meerbeke 2021; Romano et al. 2010; Lorca et al. 2020). Noonan syndrome with multiple lentigines is a more sever disease, the rate of which is unknown (Lorca et al. 2020). The mutations found in Shp2 in Noonan syndrome with multiple lentigines are loss of function mutations (Orrego-González, Martin-Restrepo, and Velez-Van-Meerbeke 2021; Romano et al. 2010; Lorca et al. 2020). Mutations in Shp2 have also been shown to be associated with leukemias as well as solid tumors (Zheng et al. 2013).

In mice, Shp2 mutations were seen to cause failure of the transition of epithelium to mesenchyme during early development. In chimeric mice with minimal Shp2 mutant cell lineage have hind limb abnormalities caused by deficient cell migration (Feng 1999). In zebrafish, there are two PTPN11 (PTPN11 a&b) genes encoding for two Shp2 (Shp2 a&b) proteins that have similar catalytic activity. Knockdown of Shp2b led to no phenotypic abnormalities in the zebrafish while mutations in Shp2a led to craniofacial abnormalities, shortened embryos, and death after 5 days. There was decreased Erk activation only in zebrafish with deletion of

both Shp2 proteins, not with deletion of a single Shp2 (Hale and den Hertog 2017). In zebrafish, Shp2 activates the MAPK pathway and inhibition of Shp2 inhibits cell growth and proliferation (Hale and den Hertog 2017). In C. elegans, PTP-2, the homologue for Shp2, is required for normal oogenesis (Feng 1999). There is only one Shp2 found in *Ciona*.

Reactive Oxygen Species

Under stress conditions, reactive oxygen species (ROS) increase within a cell due to an increase in cellular metabolism. In marine species, seasonal temperature changes cause changes in cellular stress seasonally as well which increase ROS production. In a species of blue crab and a species of clam it was seen that during the summer months, where the water temperature is highest and cellular stress is causing increased ROS, there was an increase in phosphorylated MapK (Feidantsis et al. 2020). In oysters, increased ROS stress due to high water temperatures leads to inhibition of the antioxidant defense system (Rahman and Rahman 2020).

ROS can reversibly bind to the catalytic site within the Shp2 PTP domain causing inhibition of the catalytic site (Meng, Fukada, and Tonks 2002). It has been shown that ROS causes oxidative inactivation of SHP2 as part of a feedback loop that leads to downstream platelet aggregation in humans (Jang et al. 2014). In planarians, ROS have been shown to be required for the activation of the Erk/MapK pathway during regeneration events (Jaenen et al. 2021).

Ciona intestinalis as Model Organism

The accumulation of greenhouse gases in the atmosphere is causing a rapid change in marine environments with a projection of a temperature rise in the ocean of as much as 4°C by the end of the century (Allison and Bassett 2015; Hare et al. 2016). To date, there is very little known about how increased temperature will affect the embryonic development of marine organisms. The ascidian *Ciona intestinalis*, a tunicate, is in the phylogenetically closest invertebrate group to the vertebrates, making them relevant to vertebrate biology, including humans (Corbo, Di Gregorio, and Levine 2001). The knowledge about embryonic development and reproductive ability at higher temperatures can also be applied to other marine organisms. *C. intestinalis* was also one of the first animals to have its genome fully sequenced. There is a lot known about the genes involved in the specific stages of embryo development in *Ciona*. *C. intestinalis* develop very rapidly, reaching the larval stage within 18 hours of fertilization, making them a good model organism for the study of marine species development in a changing environment. It has also been found that many genes of *Ciona intestinalis*, especially the ones expressed during the larval stage, have molecular homologies with the genes expressed during development in vertebrates (Takahashi et al. 1999).

Temperature Effects on Development in Ciona

Embryogenesis is a sensitive process in which cell-cell signaling and cell motility is extremely important. Previous research in the Irvine lab has shown that in *Ciona intesintalis*, as temperature increases, the ability to have normal

embryogenesis falls sharply between 23°C, where there is about 60% normal embryogenesis, and 24°C, where there is about 10% normal embryogenesis. Embryos reared between 19 and 25°C were categorized into 4 developmental phenotypes (Table 1). As temperature increases, the proportion of embryos with severe developmental abnormalities increases as well (Irvine et al. 2019).

Table 1: Characterization of 4 developmental phenotypic categories of *Ciona intesintalis* embryos as observed under temperature stress(Irvine et al. 2019)

Phenotype	Nickname	Specific late stage characteristics
Type I	normal	Typical wild type late tailbud: tail – straight notochord, 20 notochord cells, straight lateral muscle bands, dorsal nerve cord, ventral endodermal strand; trunk – 3 palps, lateral atrial rudiments, dorsal sensory vesicle with 2 pigment cells, etc.
Type II	kinked tail	Trunk similar to Type I; tail with 20 notochord cells but shorter due to partial failure of extension, and with abnormal kink(s)
Type III	deformed tail	Failure to progress to normal late stage trunk morphology; notochord cells fail to fully extend, resulting in much shorter curled tail
Type IV	globular	Highly anomalous trunk morphology, including abnormal position of pigment cell(s), lack of clear sensory vesicle, abnormal overall shape; complete failure of extension of notochord cells result in disorganized tail anatomy

2.2 Materials and Methods

Biological Materials

Gravid *C. intestinalis* adults were collected from Point Judith Marina in South Kingstown, Rhode Island between May and October with a small hiatus during August when the water is at its hottest. Animals were placed in an aquarium under constant light for 36 to 48 hours after collection to allow for the animals to store gametes.

Oocyte Collection

As *Ciona intestinalis* are hermaphroditic, eggs and sperm were collected from two separate animals for fertilization. The outer tunic was removed in order to

expose the inner tunic which was cut away to expose the muscle layer. Once the muscle layer is exposed, the oviduct and sperm duct are identified, and a small incision is made in the muscle layer to allow access to the oviduct and sperm duct. Once exposed, a tungsten needle is used to poke a small hole in the oviduct to allow for the eggs to flow out without coming into contact with any sperm. A P1000 pipettor is used to remove the eggs from the hole in the oviduct and place them in a dish containing a mesh screen (to keep the eggs in one location) and filtered seawater. Once all the eggs were collected, they were washed with filtered sea water to ensure no debris was left. Eggs are then aliquoted into the dishes for each experimental condition.

Fertilization

A fresh, gravid *C. intestinalis* is dissected and the sperm is collected in the same manner that the eggs were. The sperm is diluted (1:100) and activated by mixing with filtered sea water. Each mesh screen dish containing eggs is fertilized using sperm from a different adult. Only a small amount of the diluted sperm (about 100µl) is added to each dish. The eggs and sperm are given 10 minutes to allow for fertilization. After 10 minutes, the eggs are washed with fresh FSW to wash away all remaining sperm.

For dechorionated oocytes, only a small amount of the diluted sperm (about 10 µl) is added to each dish as the chorion has been removed so the chances of polyspermy increases. The eggs and sperm are given 10 minutes to allow for fertilization. After 10 minutes, the eggs are collected at the center of the dish and

transferred to a new dish. This ensures that as little sperm is left in the dish while embryogenesis begins.

Shp2 Inhibitor (NSC-87877)

A Shp2 protein tyrosine phosphatase inhibitor 8-hydroxy-7-(6-sulfonaphthalen-2- yl)41iazinyl-quinoline-5-sulfonic acid (NSC-87877) (Chen et al. 2006) (Calbiochem 565851) was used to block the phosphatase activity of the Shp2 protein.

Fluorescent Staining

Embryos were reared at 18°C either in control sea water or sea water containing 35μM Shp2 inhibitor for 12 hours. Embryos were then fixed in 4% paraformaldehyde in Ca/Mg-free seawater for 30 minutes. Embryos were then washed 4 times with phosphate buffered saline with 1% Tween-20 (P-Tween). Embryos were then permeabilized by washing once PBS containing 0.02% Triton X-100 with 50 mM ammonium chloride (PBST2-A) and then once again with PBST2-A and gently rocked for 30 minutes at room temperature. 2 μl of 40x (66μM) Phalloidin-AlexaFlour 546 (Invitrogen A22283) stock was redissolved in 250 μl of PBS containing 0.02% Triton X-100 (PBST2) per batch of embryos. 5 mg/ml DAPI (Molecular Probes D-1306) stock was diluted 1:10 in phosphate buffered saline containing 0.02% Triton X-100 (PBST2) and added to the phalloidin working solution to generate a 2X staining solution (2μg/ml DAPI and 0.5μM Phalloidin). The staining solution is added 1:1 into embryos and embryos were covered and rocked at room temperature for 2 hours. After the staining was complete, embryos were washed

once for 5 minutes in phosphate buffered saline containing 0.01% Triton X-100 (PBST1) and then washed twice for 15 minutes in phosphate buffered saline (PBS).

Fluorescent Imaging

Embryos were placed onto a silanized microscope slide. The embryos were held in place on the slide by small pieces of coverslip glass that had been glued to either side of the slide to prevent crushing the embryos. Embryos were imaged in PBS.

Hydrogen Peroxide (H_2O_2) as Oxidative Stress

H_2O_2 was used to mimic the increase in oxidative stress in increasing water temperature. *Ciona* embryos were reared at a control temperature of 18°C at a control of 0 µM H_2O_2, at 50 µM H_2O_2 and at 100µM H_2O_2. Embryos were allowed to develop for 18 hours at which, in normal development, the embryos could hatch out of the chorion as swimming larva. If embryos were not hatched, they were chemically dechorionated to allow for observation of morphological differences.

Dechorionation

Petri dishes were coated with 0.1% gelatin with 0.1% formaldehyde and washed. Seawater was filtered using a 0.2 µm filter to remove microbes. A 1% sodium thioglycolate solution at pH 10.1-10.3 with 2mg/ml protease (Sigma P5147) is used to remove the chorion from the oocytes. Once approximately 50% of the chorions had fallen off the oocytes, the reaction was quenched using 1mM glycine in FSW. 20 U Penicillin/20 µg Streptomycin per ml of seawater was added to the seawater for rearing each experimental condition.

The eggs were then transferred to the 60mm dish containing only sodium thioglycolate, mixed, and allowed to settle to the bottom. The eggs were then transferred to the 60mm dish containing sodium thioglycolate with protease where they were swirled and shaken in the dish under close watch in the dissecting scope. The eggs stayed in with the protease for 2-3 minutes, until the chorions of about ¼ of the eggs had fallen off. Once this was seen, the entire dish was dumped into the "prep" dish containing glycine in order to quench the protease and stop the digestion of the proteins in the chorion. The eggs, now with chorions removed or falling off, are washed with filtered sea water until all of the chorion debris in the water is removed. Eggs are then dispersed into the dishes for each experimental condition to pre-incubate for 2 hours at 15, 18, or 22°C.

Temperature and Shp2 Inhibitor Chase Experiment

After dechorionation, pre-incubation, and fertilization, embryos were challenged with either temperature stress alone or temperature stress in conjunction with Shp2 inhibition for either the first 3 hours, hours 3-6, or hours 6-12 of embryological development. Embryos were pre-incubated prior to fertilization under the experimental conditions the embryos would spend the first 3 hours of development. Control embryos were kept at 15°C for the entirety of development as this was the control temperature for the environment at the time of year this experiment was conducted. Half of the embryos kept at 15°C for development were exposed to 25 µM Shp2 inhibitor for either 0-3 hours, 3-6 hours, or 6-12 hours of development, after which the inhibitor was washed out. 18°C was used as a mild

temperature stress and 22°C was used as an extreme temperature stress for embryological development. A proportion of the embryos were subjected to either 18°C or 22°C for either 0-3 hours, 3-6 hours, or 6-12 hours of embryological development. Half of the embryos subjected to temperature stress were also subjected to 25 µM of Shp2 inhibitor during the same time range of development after which the inhibitor was washed out and the embryos were brought back to the control temperature of 15°C.

RNA Extraction

Total RNA was extracted from embryo samples using the RNA XS kit (Marcherey-Nagel 740902.50) and the total RNA was frozen at -80°C as quickly as possible. RNA was quantified by spectrophotometry.

cDNA Preparation

The preparation of cDNA began with the standardization of the RNA concentration used for each cDNA preparation. 200ng of RNA was used with the New England BioLabs ProtoScript First Strand cDNA Synthesis Kit. According to the manufacturer's instructions the RNA was mixed with SR-Poly-T primer (non-specific primer that will bind to the Poly-A tail on mRNA) and dNTPS and incubated at 65°C for 5 minutes then put on ice. The reaction mixture of reverse transcriptase buffer, $MgCl_2$, DTT, and RNAse inhibitor were then added, and each sample was incubated at 45°C for 2 minutes. 1 µl of reverse transcriptase (RT) enzyme (Protoscript II NEB M0368) was added to each sample, with the exception of the no RT control, and incubated at 45°C for 50 minutes. The reaction was inactivated by incubating at 70°C

for 15 minutes and then the samples were put on ice. 1 µl of RNAse H was added to each sample and was incubated at 37°C for 20 minutes. Samples were stored at -20°C until use in RT-PCR reactions.

Semi-quantitative RT-PCR

cDNA was amplified using gene specific primers to do semi-quantitative analysis of gene expression of embryos (gastrula stage and tailbud stage) that developed at 18, 22, and 23°C. Each 20 µl RT-PCR reaction was a mixture of 1 µl template cDNA, 1 µl forward primer (10 µM), 1µl reverse primer (10 µM), 4 µl 5X Phusion buffer, 0.4 µl dNTPs (10 mM), and 0.2 µl Phusion DNA Polymerase. The RT-PCR samples were place into the thermocycler once the block was preheated to 80°C. The thermocycler ran an initial denaturation for 2 minutes at 94°C and 35-40 amplification cycles consisting of a 30 second denature at 94°C, a 30 second anneal at the temperature specified for each primer, and an extension for 1 minute/kb of product at 72°C. RT-PCR product were then run via gel electrophoresis on a 1% agarose gel and imaged.

Gel Analysis of RT-PCR

ImageJ was used to analyze the results of the RT-PCR products run on a 1% agarose gel. The bands were analyzed using the gel analysis tool for density.

2.3 Results

Shp2 Inhibitor Concentration

In order to determine the concentration of Shp2 inhibitor that has an effect on embryogenesis in *C. intestinalis*, a titration experiment was performed, rearing

embryos at multiple concentrations of Shp2 inhibitor. *Ciona* were reared at a control temperature of 18°C with Shp2 inhibitor concentration ranging from 5µM to 45µM (Figure 10). At concentrations of Shp2 inhibitor 15 µM and below, there was over 70% normal development of embryos (Type I embryos) with a small increase in the mean percentage of Type II to just above 20% at 15 µM Shp2 inhibitor. At 25 µM Shp2 inhibitor, the mean percent of Type I embryos drops to below 50% and there is an increase in both Type II and Type III/IV embryos. At 35 µM Shp2 inhibitor, the mean percent of Type I embryos drops below that of both Type II and Type III/IV embryos. At 45 µM Shp2 inhibitor, the mean percent of Type III/IV increases above that of both Type I and Type II embryos. The mean percent of Type II embryos increases beginning at 15 µM Shp2 inhibitor until becoming the most prevalent phenotype seen at 35 µM Shp2 inhibitor. The mean percent of Type III/IV embryos increases beginning at 25 µM Shp2 inhibitor until becoming the most prevalent phenotype seen at 45 µM Shp2 inhibitor.

Shp2 Inhibitor at 35µM

35 µM Shp2 inhibitor showed the most similar pattern of phenotypic variation to embryos reared at high stress temperatures. In order to elucidate the role of Shp2 in embryonic development, *C. intestinalis* embryos were reared with 35 µM Shp2 inhibitor (NSC-87877) in FSW while control embryos were reared in normal FSW. When embryos were reared with 35 µM of Shp2 inhibitor (Figure 11 B-H) the phenotypes of the embryos mimic the phenotypes seen in embryos reared at high stress temperatures (Irvine et al. 2019) as compared to control embryos not reared

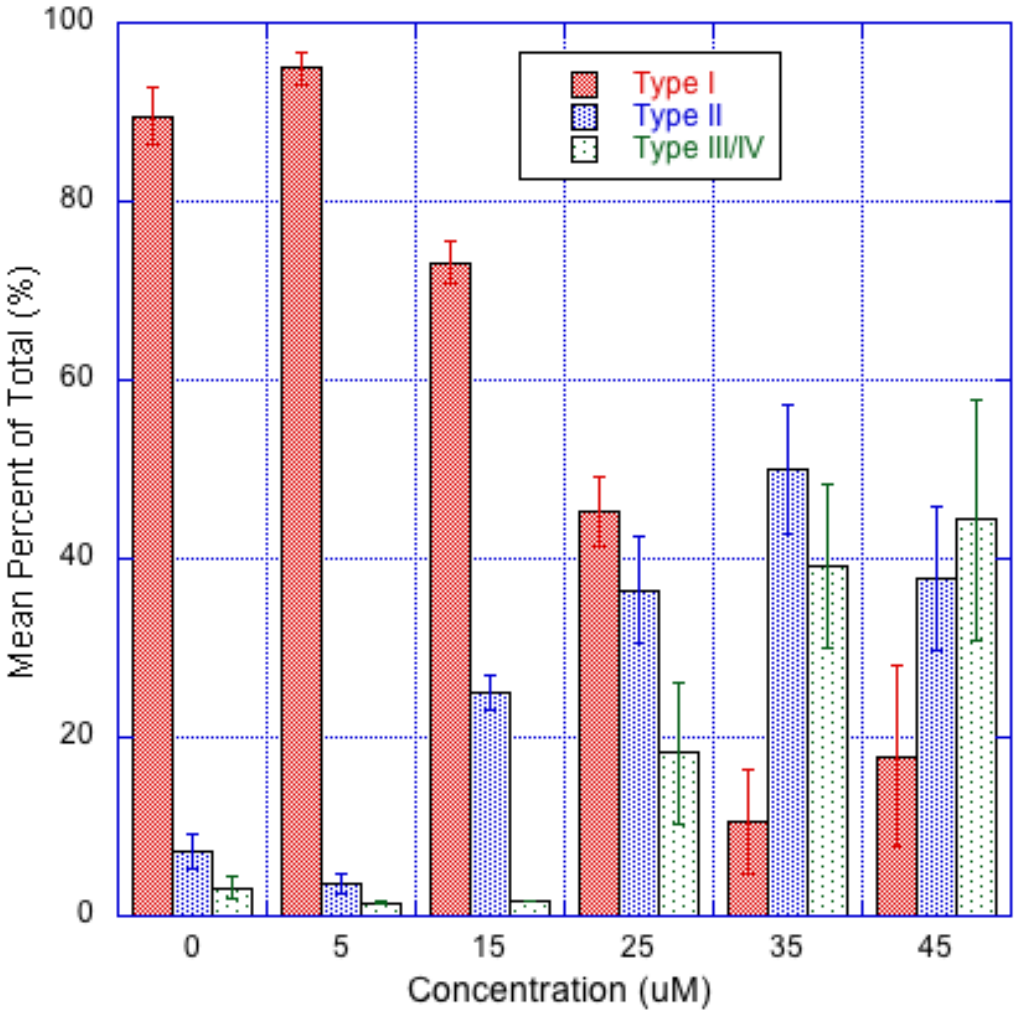

Figure 10: Mean percent of total embryo phenotype reared in Shp2 inhibitor concentrations from 0-45 µM at 18°C

with Shp2 inhibitor (Figure 11 A). All four types of embryos (as described in Table 1) were seen in the embryos reared in 35 µM Shp2 inhibitor. There were deformations seen in the tail, typically the milder deformations that happen during embryogenesis, characterized by kinks in the notochord (solid white triangles in D, E, & F) as well as radial pinching of the notochord (white outline triangle in C). There were also more extreme deformations where the notochord cells fail to extend fully, and the morphology of the larval trunk is abnormal (Figure 10 G & H). In all embryos, the

pigment cells were present which are generated at the latest embryonic stages, although not always in the correct location, meaning late-stage cell type specification is occurring correctly.

Figure 12 shows examination of the tail morphology in embryos reared with 35µM Shp2 inhibitor (Figure 12 B-H) as compared to the tail morphology in a control embryo (Figure 12 A). Normal tail morphology, as seen in control embryos (Figure 12 A), has complete extension of the notochord within the tail epidermis so that the tail is straight by larval stage of embryological development. Figure 12 B-E show the kinks in the notochord that are commonly seen in embryos reared with Shp2 inhibitor. The kinks in the notochord vary from mild curvatures (Figure 12 B & D) to sharp angle curvatures (Figure 12 C & E). This same variation of notochord curvatures was seen in embryos reared under temperature stress(Irvine et al. 2019). One unique tail morphological difference seen in embryos reared at 35µM Shp2 inhibitor was a radiating pinching of the notochord (Figure 12 F). Embryos reared with 35µM Shp2 inhibitor also showed lack of notochord extension leading to shortened tail morphology (Figure 12 G & H).

Figure 13 shows examination of the trunk morphology in embryos reared with 35µM Shp2 inhibitor (Figure 13 B-H) as compared to the morphology in a control embryo (Figure 13 A). Normal trunk morphology, as seen in control embryos, has thickening and extension of the trunk epithelium at the anterior surface into three palps. Mild trunk morphological deformations in embryos reared in the presence of 35µM Shp2 inhibitor are shown in Figure 13 B, C, & D. Embryos reared in the

presence of Shp2 inhibitor had trunk morphology that lagged behind in the developmental timeline (Figure 13 B) as compared to their control counterparts. The development and location of the pigment spots are correct but the extension of the trunk epithelium into the palps is delayed (Figure 13 B) as compared to the control counterparts (Figure 13 A) which were reared for the same length of time. Embryos reared in the presence of Shp2 inhibitor also had asymmetrical extension of the trunk epithelium (Figure 13 C, D, & G). Extension of the trunk epithelium on the ventral (Figure 13 C) or dorsal (Figure 13 D & G) surface exclusively would cause irregular palp formation. Improper yet symmetrical extension of the trunk epithelium also occurred in embryos reared in the presence of Shp2 inhibitor (Figure 13 E, F, & H). A singular point of extension where the cells do not come to a point on the anterior end of the extension (Figure 13 E) as well as a singular point of extension with globular rather than elongated cell shape (Figure 13 H) were both seen.

Normal trunk morphology, as seen in control embryos (Figure 13 A), has two pigment spots, one otolith and one ocellus, that are antero-posteriorly oriented to one another. Abnormal orientation of the pigment spots (the otolith and ocellus) occurred in embryos reared in the presence of Shp2 inhibitor (Figure 13 C, E, F, G, & H). Pigment spots in embryos reared in the presence of Shp2 inhibitor were closer together than pigment spots in control embryos while still oriented antero-posteriorly to one another (Figure 13 C, F, G, & H). In other embryos, pigment spots were located farther from one another as compared to control embryos (Figure 13 E).

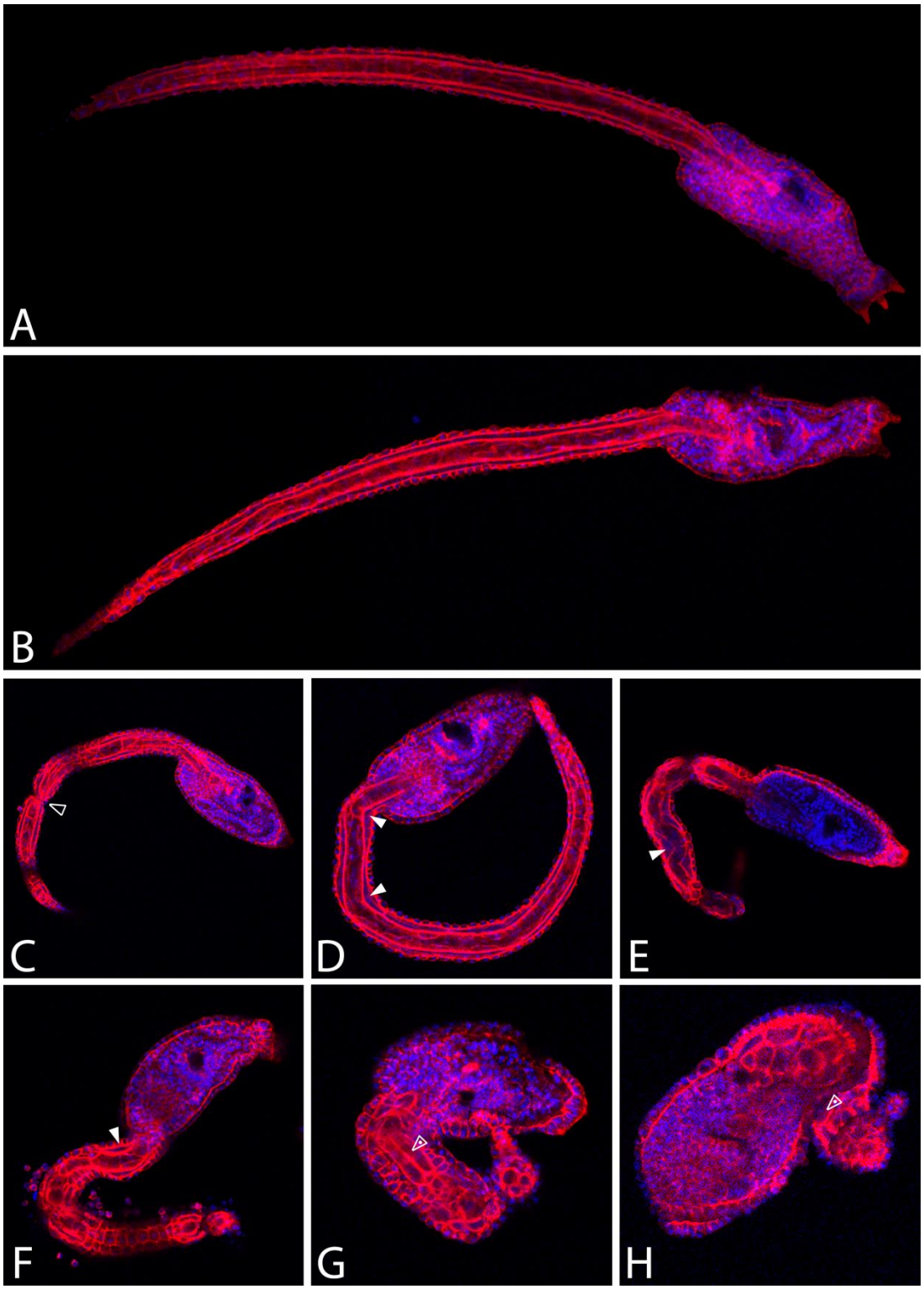

Figure 11: 4 phenotypes of embryos observed when reared in the presence of 35µM Shp2 inhibitor A: Control embryo; B-H: Embryos reared in the presence of 35µM Shp2 inhibitor; B&C: Type I Embryos D&E: Type II Embryos F: Type III Embryo G&H: Type IV Embryos

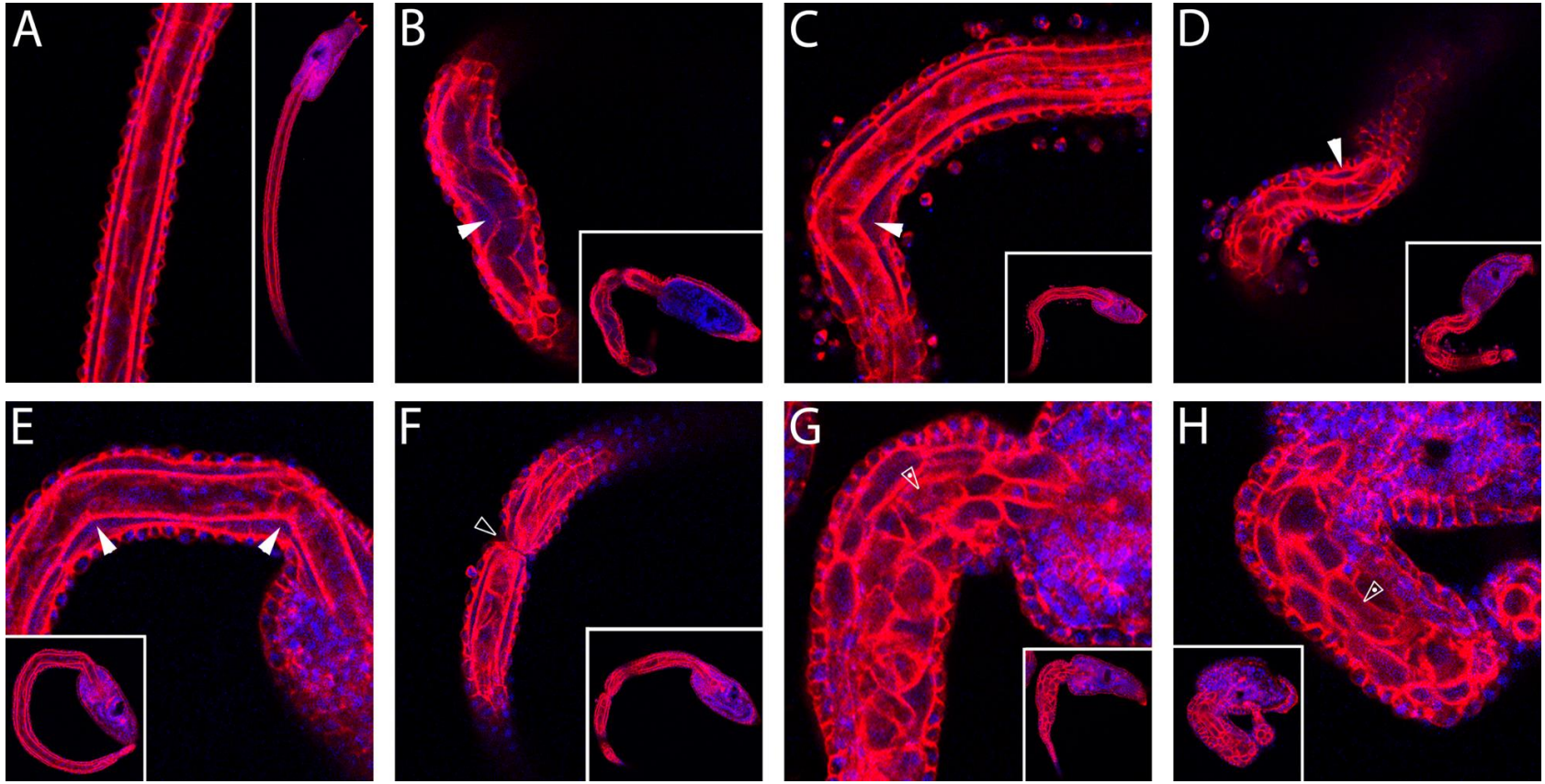

Figure 12: Tail morphology of embryos reared in the presence of 35µM Shp2 inhibitor A: Control embryo B-H: Embryos reared in the presence of 35µM Shp2 inhibitor. Solid arrows indicate kinks in notochord. Hollow white arrows indicated radial pinching of notochord. Hollow white arrows with white dot indicate improper organization of notochord.

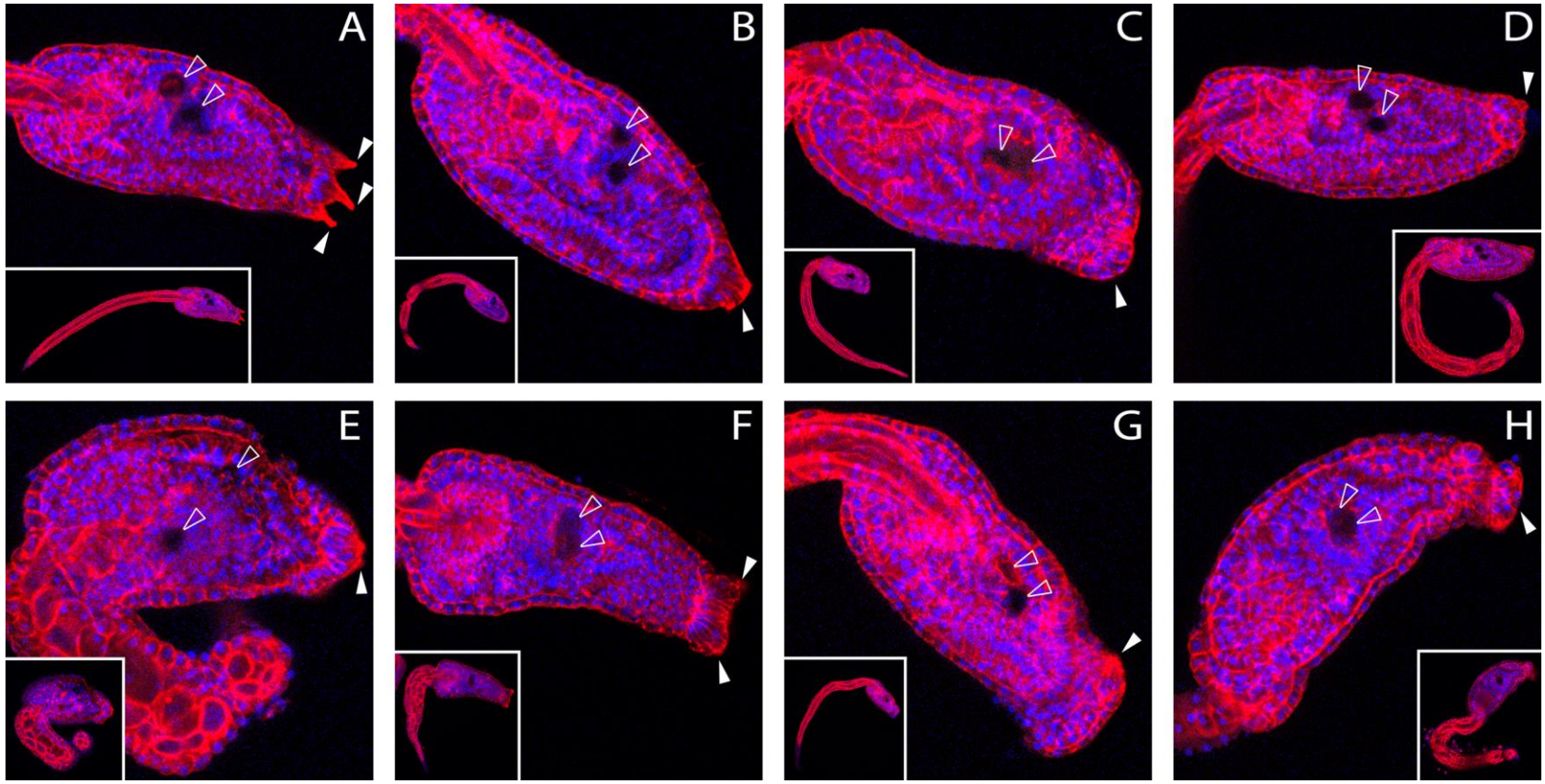

Figure 13: Trunk morphology of embryos reared in the presence of 35µM Shp2 inhibitor A: Control embryo B-H: Embryos reared in the presence of 35µM Shp2 inhibitor. Solid white arrows indicate extensions of trunk epithelium. White arrow outlines indicate pigment spots.

Hydrogen Peroxide (H_2O_2) as Oxidative Stress

Ciona intestinalis embryos were reared with differing concentrations of H_2O_2 to assess if increased concentrations of reactive oxygen species would result in the same phenotypic patterns as seen at increased temperature and Shp2 inhibitor. Figure 14 shows that at 50 µM H_2O_2 there was about 30% normal development and 70% abnormal development. At 100µM H_2O_2 there was less than 10% normal development, about 20% abnormal development with the ability to hatch, and over 60% abnormal development with the inability to hatch. At 0 µM H_2O_2, the control concentration, all four phenotypes described in Table 1 could be seen with a bias towards normal, type I embryos. At 50 µM concentration of H_2O_2 the percent of normal, type I embryos began to drop while the percent of type II and type III/IV embryos began to increase. At 100 µM H_2O_2 all four of the phenotypes described in Table 1 could be seen with a bias towards type III and IV phenotypes.

Figure 15 shows examples of each phenotype found at 100 µM H_2O_2. All of the phenotypes seen at 100 µM H_2O_2 are consistent with the phenotypes seen at high temperature stress (Irvine et al. 2019) as well as the phenotypes seen with 35 µM Shp2 inhibitor (Figure 11). Type I embryos (Figure 15 B), although they could be found, were sparse. They exhibited typical morphological traits that were also seen in the control embryos (Figure 15 A). In the Type I embryos (Figure 15 B) the tail was fully extended with intercalating notochord cells completely encased in the tail epidermis. The trunk was fully extended with thickening of the anterior epithelial surface (the beginning of palp formation). There were also two pigment spots located

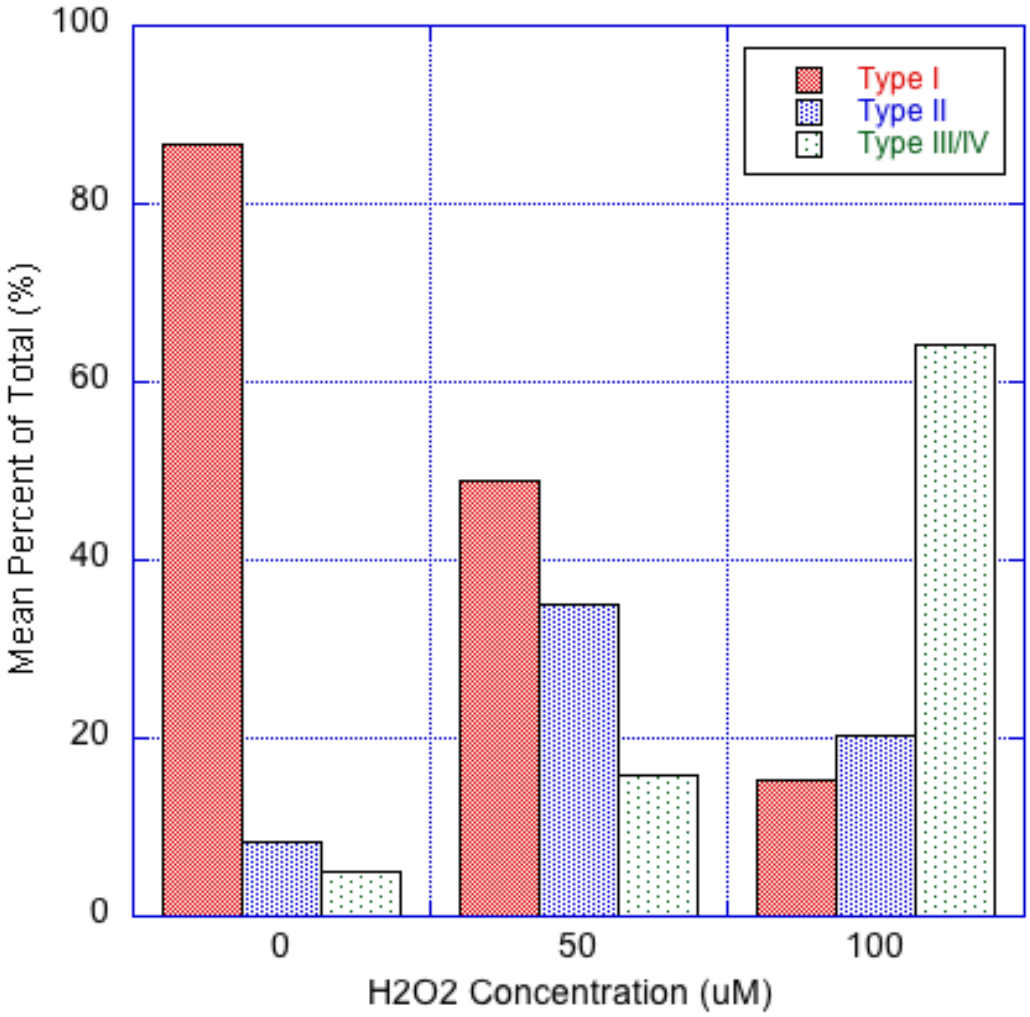

Figure 14: Mean percent of total embryo phenotype reared H_2O_2 concentrations from 0-100 µM at 18°C

along the anterior-posterior axis. Type II embryos (Figure 15 C) were seen at a slightly higher proportion at 100 µM H_2O_2 and were characterized by mild tail deformations. There were kinks in the tail ranging from mild curvatures to sharp angles while the trunk morphology was typical of a normal embryo. At 100 µM H_2O_2 the majority of the embryos were Type III (Figure 15 D & E) and Type IV (Figure 15 F). The Type III embryos (Figure 15 D & E) were characterized by multiple kinks in the tail and lack of extension of the trunk. There was still late-stage cell type specification to allow for

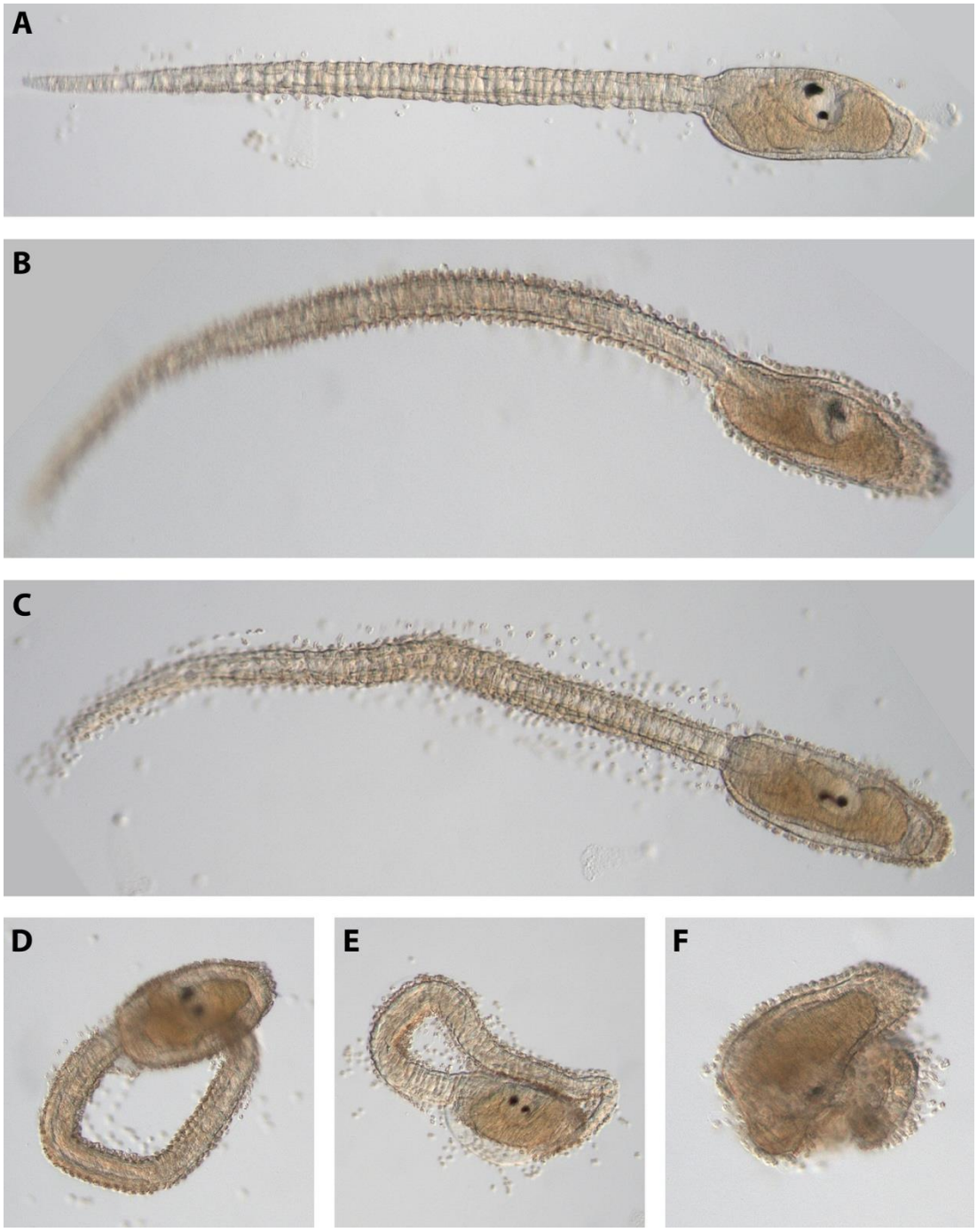

Figure 15: 4 phenotypes of embryos observed when reared in the presence of 100µM H_2O_2 A: Control embryo; B-H: Embryos reared in the presence of 100µM H_2O_2; B: Type I Embryo C: Type II Embryo D&E: Type III Embryos F: Type IV Embryo

the formation of the two pigment spots and the location of the spots are in the proper orientation in relation to one another. The Type IV embryos (Figure 15 F) were characterized by lack of extension of the tail, abnormal trunk morphology, and while the pigment spots were present, they were in abnormal locations. These results are consistent with the morphological abnormalities seen with Shp2 inhibition as well as temperature stress (Irvine et al. 2019).

Shp2 Inhibition and Temperature Stress

This chase experiment was used to determine which stages of embryogenesis are most sensitive to Shp2 inhibitor, and if the combination of Shp2 inhibitor and temperature stress would compound the effects that they have on embryogenesis individually. Figure 16 A3 and B3 show tailbud stage embryos and both A3 and B3 are classified as type I, normal, embryos with no abnormalities. Figure 16 C3 and D3 show tailbud stage embryos and C3 is classified as a Type I, normal, embryo while D3 is classified as a Type II embryo, with an exaggerated bend in the tail. Figure 16 E3 and F3 show tailbud stage embryos and both E3 and F3 are classified as Type IV embryos, with globular conformations, lack of tail extensions, and severe trunk abnormalities.

The control embryos (15˚C) at tailbud stage (Figure 16, A5 and B5) are characterized as Type I, normal, embryos. The mild temperature stress embryos (18˚C) at tailbud stage (Figure 16, C5 and D5) are characterized as Type I, normal, embryos. The high temperature stress embryos (22˚C) at tailbud stage (Figure 16, E5 and F5) are characterized as type II and type IV embryos, respectively. Figure 16 E5 is

characterized as a Type II embryo with a slight exaggeration in the bend of the tail. Figure 16 F5 is characterized as a Type IV embryo, with kinks in the tail as well as lack of full tail extension and abnormal trunk morphology.

The control embryos (15˚C) at tailbud stage (Figure 16, A6 and B6) are characterized as Type I, normal, embryos. The mild temperature stress embryos (18˚C) at tailbud stage (Figure 16, C6 and D6) are characterized as Type I, normal, embryos. The high temperature stress embryos (22˚C) at tailbud stage (Figure 16, E6 and F6) are characterized as Type I, normal, embryos.

Shp2 Gene Expression in Embryos

Semi-quantitative RT-PCR was used to determine if transcript expression patterns of Shp2 changed with temperature stress and at different stages of embryogenesis. Figure 17, the gel electrophoresis analysis of RT-PCR products, shows there is increased Shp2 transcript expression at gastrula stage embryos as compared to tailbud stage embryos. As the rearing temperature increases, the expression of Shp2 transcripts also increases. Actin serves as a loading control for the RT-PCR while the negative control contained no cDNA.

Figure 18 shows densitometry analysis of the Shp2 RT-PCR bands. The densitometry showed that Shp2 transcript expression in gastrula stage embryos is significantly higher than that in tailbud stage embryos (P-value 0.0122). When normalized to Shp2 transcript expression in the ovary, the most upregulation was seen in the 23°C gastrula stage embryos. The least upregulation of Shp2 transcript expression was seen in 23°C tailbud stage embryos.

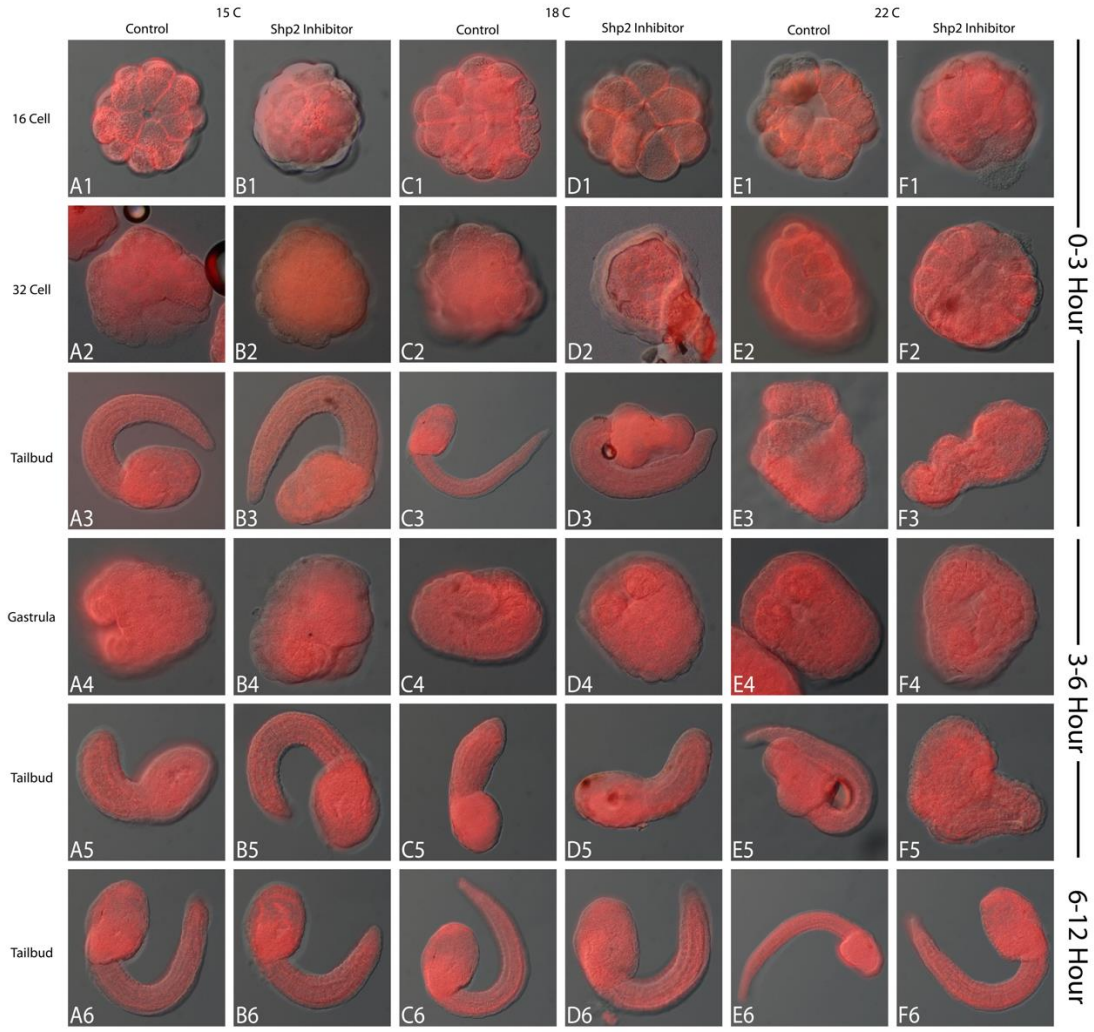

Figure 16: Shp2 inhibition vs temperature chase embryos. Columns A, C, and E are control embryos that were only subjected to temperature stress while columns B, D, and F are embryos that were subjected to Shp2 inhibitor along with temperature stress. Columns A and B were the temperature control embryos, being kept at 15°C for the entirety of development. Columns C and D, the embryos were subjected to slight temperature stress at 18°C for the time periods of development specified on the right had side of the table. Columns E and G, the embryos were subjected to high temperature stress at 22°C for the time periods of development specified on the right had side of the table. The left-hand side of the table is the stage of development that the image was taken at.

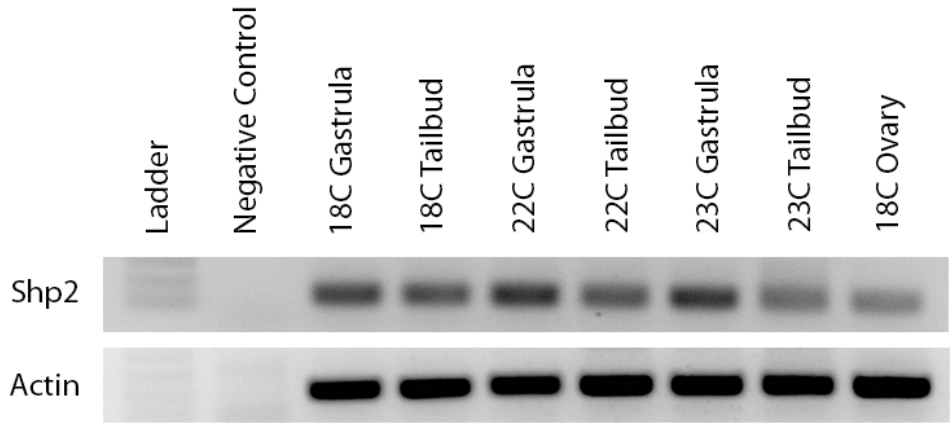

Figure 17: RT-PCR results using Actin and Shp2 primers, PCR was run for 30 cycles at an annealing temperature of 65°C

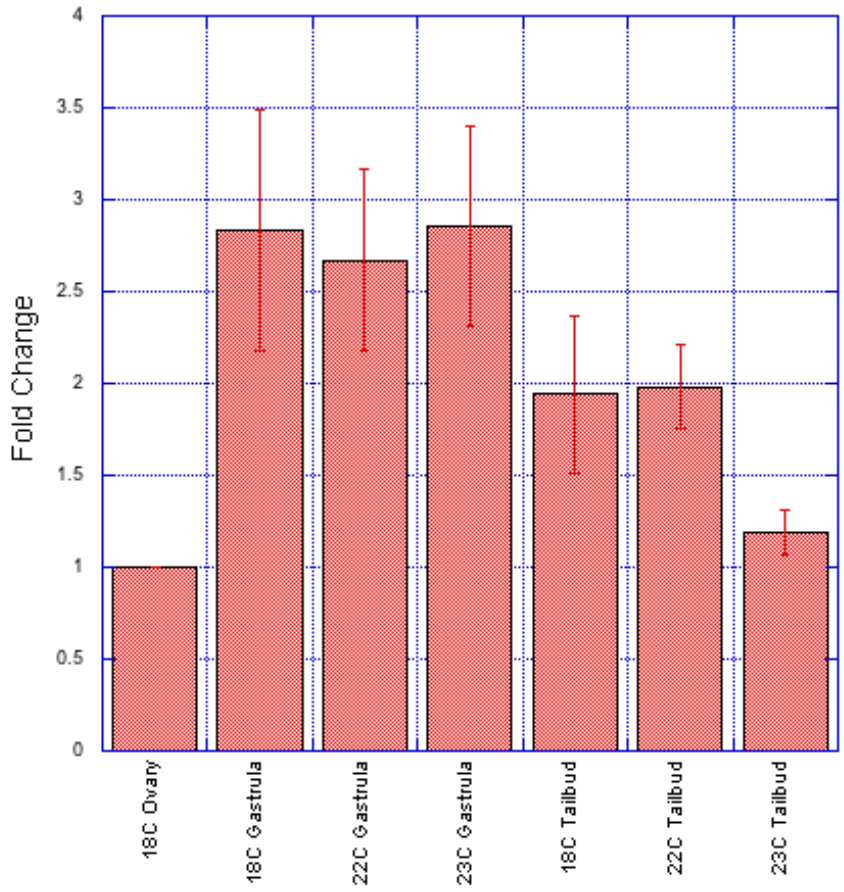

Figure 18: Densitometry analysis of RT-PCR for fold change of Shp2 transcript expression as compared to ovary expression in gastrula and tailbud stage embryos reared at different temperatures.

2.4 Discussion

Shp2 Inhibitor Concentration

Species survival and propagation is dependent upon proper embryogenesis and maturation to sexual maturity. In *Ciona intestinalis*, propagation is dependent upon proper embryogenesis in the majority of the fertilization events. As seen in our lab experiments, as temperature increases normal embryogenesis declines sharply (Irvine et al. 2019). As outlined above, Shp2 protein is hypothesized to be important in modulating the developmental response to high temperature. To verify that Shp2 is important to the stress response, a Shp2 inhibitor, NSC-87877, was used to block the dephosphorylation site of the Shp2 protein. NSC-87877 has been shown to reduce Shp2 activity in HEK293 cells by 97% at a concentration of 50 μM (Chen et al. 2006). The Shp2 inhibitor binds to the catalytic site of the protein, making the Shp2 protein no longer able to dephosphorylate proteins (Tajan et al. 2015; Chen et al. 2006; Hale and den Hertog 2017).

Below 25 μM Shp2 inhibitor, there are more than 50% average Type I embryos (Figure 10) which is consistent with the phenotypic variation seen over the range of reproductively successful temperatures in our lab experiments. At 25 μM Shp2 inhibitor and above, the mean percent of Type I embryos quickly declines, and the abnormal embryo phenotypes (Type II and Type III/IV) begin to become more prevalent. Type II embryos, characterized by kink and bends in the tail, peak at 35 μM Shp2 inhibitor. Type III/IV embryos, characterized by lack of tail extension and/or globular shape, peak at 45 μM Shp2 inhibitor (Figure 10). Above 15 μM Shp2

inhibitor, the embryos, which normally have the ability to hatch out of their chorion because of the movement of their tail, were no longer able to hatch out of their chorion. If they were able to hatch out of their chorion, the kinks and abnormal tail morphology did not allow for the embryos to swim properly. This data suggests a dose dependent effect of the Shp2 inhibitor on the normal embryogenesis of *C. intestinalis*.

Shp2 Inhibitor at 35 μM

As embryogenesis proceeds in *Ciona intestinalis*, extension of the tail begins at the tailbud stage and continues until hatching from the chorion at the larval stage. As extension of the tail occurs the notochord is extending within the surrounding tail epidermis. In normal tail development, the extension of both the notochord and tail epidermis occur at the same rate allowing for, by the time the larva hatches, the tail to be straight so the larva can swim properly. When embryos develop in the presence of Shp2 inhibitor, the tail does not develop properly, there are curves and kinks that would inhibit the ability of the larva to swim properly (Figure 11).

When examining more closely the tail morphology of the embryos reared in the presence of Shp2 inhibitor (Figure 12), it may be that the extension of the notochord cells is occurring at a faster rate than the extension of the tail epidermis causing the notochord to bend and kink within the tail. It may be that Shp2, as it is responsible for not only signal transduction from external signals but also signal transduction between cells (Tajan et al. 2015; Feng 1999; Neel, Gu, and Pao 2003), is responsible for signaling cells in the tail during extension of the notochord and tail

epidermis. Inhibition of Shp2 signaling with the Shp2 inhibitor may not allow for the signaling between cells to occur as it should. This may cause the cells to lose their coordination when it comes to extension which would cause kinks in the tail.

In order for proper attachment to a substrate, larval *Ciona intestinalis* normally have three palps that extend from the anterior surface of the trunk. The palps serve to inspect substrates, adhere to a suitable substrate, and initiate metamorphosis into the adult form (Zeng et al. 2019). When examining more closely the trunk morphology of embryos reared in the presence of Shp2 inhibitor (Figure 13), in some cases, the palps were developing improperly. There was failure of complete extension of the trunk epithelium as well as asymmetry in the extensions. Incomplete extension would lead to palp deformations.

Hydrogen Peroxide (H_2O_2) as Oxidative Stress

Increased H_2O_2 concentrations was used to simulate the increase in oxidative stress that the *C. intestinalis* embryos were under during embryogenesis at high temperatures. Analysis of the different abnormalities seen in embryos reared in 100 µM H_2O_2 (Figure 15) suggests that similar, although seemingly not as severe, defects were seen as compared to both temperature stress and Shp2 inhibition. These defects seem less severe because it looks as though the H_2O_2 affects the tail of the embryos more so than the trunk. Although the trunk seems to be less affected, this could be simply because the concentration of H_2O_2 was too low to show the same morphological abnormalities as are seen with temperature stress and Shp2

inhibition. Taken together these experiments suggest that deformation in embryogenesis seen at high temperature stress are due to increased oxidative stress.

Shp2 Inhibition and Temperature Stress

I am proposing that Shp2 helps manage the effects of increasing reactive oxygen species under temperature stress. In order to determine if Shp2 inhibition in conjunction with temperature stress would compound the effects on embryogenesis of both, embryos were subjected to temperature stress with and without Shp2 inhibition during specific time periods of embryogenesis. Temperature stress in developing *Ciona* embryos causes the most abnormalities when it occurs during the first 3 hours of embryogenesis (Figure 16). When Shp2 inhibitor (25µM) is added to the temperature stress at different developmental time points, there is a similar but exaggerated pattern of developmental abnormalities, the most of which occur when Shp2 inhibitor is present during hours 0-3 of development and the embryos are at 22°C (extreme stress temperature). At the low control temperature of 15°C there was no difference between the embryological development of control embryos and embryos subjected to Shp2 inhibitor (Figure 16 columns A & B). As seen in the titration experiment, at 25 µM Shp2 inhibitor there will still be over 50% normal embryological development. Together with Figure 16 columns A & B the results of both experiments show that Shp2 may not be required for normal embryogenesis at control temperatures.

When a mild temperature stress of 18°C (Figure 16 column C) is added in conjunction with the stress of Shp2 inhibition (Figure 16 column D), there is

exacerbation of the temperature stress by the addition of the Shp2 inhibitor for hours 0-3 of development as seen by abnormal embryogenesis in Figure 16 D3. This addition of the Shp2 inhibitor only affected embryos exposed to mild temperature stress for the first 3 hours of development (Figure 16 D1-3). When embryos were exposed to Shp2 inhibitor and mild temperature stress for hours 3-6 of development (Figure 16 D4-5) and hours 6-12 (Figure 16 D6) there were no morphological changes the embryos from normal. This suggests that the first 3 hours of development are more sensitive to the Shp2 inhibitor than hours 3-12. This was consistent with the findings that embryos are more sensitive to temperature stress in the first 3 hours of development (Irvine et al. 2019). This suggests that at this mild temperature stress, Shp2 is required to ameliorate the temperature stress to allow for normal embryogenesis.

When high temperature stress of 22°C (Figure 16 column E) is added in conjunction with Shp2 inhibition (Figure 16 column F), there is abnormal development under both the control conditions and Shp2 inhibitor conditions. When exposed to high temperature stress for the first 3 hours of development alone (Figure 16 E1-3) and in conjunction with the Shp2 inhibitor (Figure 16 F1-3) caused abnormal embryogenesis. There is a lack of tail extension as well as abnormal trunk morphology in the larva stage embryos (Figure 16 E3 & F3). This again is consistent with the findings that embryos are more sensitive to temperature stress in the first 3 hours of development (Irvine et al. 2019). It is unclear if exposure to the Shp2

inhibitor exacerbated the effects of temperature stress on embryogenesis because both embryos E3 and F3 show extreme morphological defects.

When embryos were exposed, during hours 3-6, to high temperature stress alone (Figure 16 E4-5) and in conjunction with Shp2 inhibitor (Figure 16 F4-5), it appears that Shp2 inhibition exacerbates the morphological abnormalities seen at high temperature stress alone. Tailbud embryos exposed to the high temperature stress for hours 3-6 show mild morphological abnormalities (Figure 16 E5) while high temperature stress in conjunction with Shp2 inhibitor cause more severe abnormalities (Figure 16 F5). Embryo E5 has a bend in the tail that is more extreme than in a normal embryo and embryo F5 shows multiple kinks in the tail, incomplete extension of the tail, and abnormal trunk morphology. This shows that addition of the Shp2 inhibitor on top of the high temperature stress causes more morphological abnormalities than just temperature stress alone when exposed to stress from hours 3-6 of development. This suggests that Shp2 is required for normal embryogenesis during the 3-6 hour time period in development at high stress temperatures. This again suggests that Shp2 is required to ameliorate the stress caused by high temperatures during development.

When embryos were exposed, during hours 6-12 of development, to high temperature stress alone (Figure 16 E6) and in conjunction with Shp2 inhibitor (Figure 16 F6), there are no morphological effects on embryogenesis. Both embryo E6 and F6 are normal tailbud stage embryos, meaning the high temperature alone and with Shp2 inhibitor do not have an effect on the ability for the embryo to develop

normally during that time range of development. This is consistent with the finding that embryos are not sensitive to temperature stress during later stages of development (Irvine et al. 2019).

Shp2 Gene Expression in Embryos

Shp2 transcript levels of embryos at different stages of embryogenesis that developed at different temperatures were analyzed via semi-quantitative RT-PCR (Figure 17). These results show that transcript levels of the Shp2 gene are higher at the gastrula stage of embryogenesis as compared to tailbud stage. These results also suggest that the transcript levels of the Shp2 gene declines at the highest temperature in tailbud stage embryos. Figure 18 confirms that Shp2 transcript levels are upregulated in gastrula stage embryos as compared to tailbud stage embryos. This finding shows evidence of upregulations, but not to the extreme levels as were seen in proteomic analysis of the ovaries of *Ciona intestinalis* reared at high temperatures (Irvine et al. 2019). These results together could suggest that increased Shp2 expression occurs in the most sensitive times and areas under stress conditions.

The beginning of embryogenesis is the most sensitive time in development wherein the embryo needs the most protection from the impacts of stress, both internal and external. During reproduction, the generation of gametes is the most sensitive part of the process. Gametes need the most protection from the impacts of stress to ensure reproductive success. As Shp2 is implicated in transduction of signals, both from external sources of stress as well as internal cellular stress (Tajan

et al. 2015; Feng 1999; Neel, Gu, and Pao 2003), it is likely upregulated in an attempt to ameliorate this stress.

In a stress situation, such as increased temperature stress, Shp2 may be upregulated in early embryogenesis to protect the developing embryo while cell specification and cell fate are determined and while crucial structures are laid out. These results are consistent with the results of the Shp2 chase experiment where it appears embryogenesis is most sensitive to inhibition in the first 6 hours of development (Figure 16). This increased sensitivity to inhibition may be due to the increased concentration of Shp2 proteins at earlier stages of development, although the RT-PCR can only suggest transcript level expression. Tail deformations caused by temperature stress causes the embryos to lose the ability to swim properly, if at all, inhibiting their ability to find a proper substrate to which they would settle and metamorphose into the adult morphology. Trunk abnormalities could negatively affect the ability of the embryo to settle onto a substrate which could in turn negatively affect the ability of the embryo to metamorphose into the adult form. I am proposing that Shp2 is functioning to ameliorate this stress in order to minimize these deformations.

2.5 Conclusions

Figure 19 shows a model for how the relationship between Shp2 and oxidative stress caused by increased temperature could be twofold: 1) oxidative stress causes ligands to bind to RTKs which activate Shp2 to cause signal transduction through the Erk/MapK pathway as well as signal transduction to neighboring cells (Feng 1999) and 2) ROS can reversibly bind to the catalytic site of Shp2 (Meng, Fukada, and Tonks 2002), rendering it inactive and unable to dephosphorylate proteins. It may be that increased oxidative stress would cause increased Shp2 expression 1) because Erk/MapK signal transduction is upregulated in response to increased stress signaling and 2) because when ROS bind to the Shp2 catalytic site, Shp2 is no longer functional in the Erk/MapK pathway and therefore must be upregulated to compensate for this inactivation. All together this suggests that there is interference between the two interactions between oxidative stress and Shp2 function. Therefore, the inhibition of Shp2 mimics the inactivation of Shp2 by ROS causing the deformation seen in embryos reared at high temperature stress.

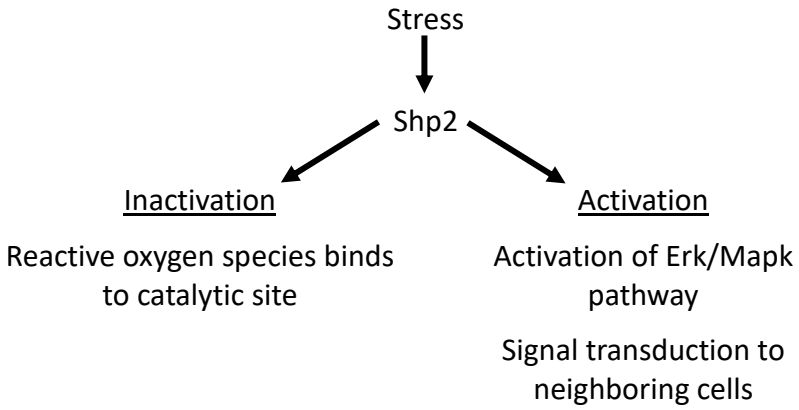

Figure 19: Hypothesized relationship between stress and Shp2 activation and inactivation

Bibliography

Achilli, Toni-Marie, Julia Meyer, and Jeffrey R Morgan. 2012. “Advances in the Formation, Use and Understanding of Multi-Cellular Spheroids.” *Expert Opinion on Biological Therapy* 12 (10): 1347–60. https://doi.org/10.1517/14712598.2012.707181.

Allison, Edward H., and Hannah R. Bassett. 2015. “Climate Change in the Oceans: Human Impacts and Responses.” *Science*. https://doi.org/10.1126/science.aac8721.

Arizza, Vincenzo, Edwin L. Cooper, and Nicolo Parrinello. 1997. “Circulating Hemocytes and Pharyngeal Explants of Styela Clava Release Hemagglutinin in Vitro.” *Journal of Marine Biotechnology*.

Ballarin, Loriano, and Matteo Cammarata. 2016. *Lessons in Immunity: From Single-Cell Organisms to Mammals*. *Lessons in Immunity: From Single-Cell Organisms to Mammals*.

Cai, X, and Y Zhang. 2014. “Marine Invertebrate Cell Culture: A Decade of Development.” *N. Oceanogr.* 70: 405–14. https://doi.org/10.1007/s10872-014-0242-8.

Chen, Liwei, Shen Shu Sung, M. L.Richard Yip, Harshani R. Lawrence, Yuan Ren, Wayne C. Guida, Said M. Sebti, Nicholas J. Lawrence, and Jie Wu. 2006. “Discovery of a Novel Shp2 Protein Tyrosine Phosphatase Inhibitor.” *Molecular Pharmacology*. https://doi.org/10.1124/mol.106.025536.

Corbo, Joseph C., Anna Di Gregorio, and Michael Levine. 2001. “The Ascidian as a

Model Organism in Developmental and Evolutionary Biology." *Cell*. https://doi.org/10.1016/S0092-8674(01)00481-0.

Corliss, John O., and Gretchen L. Humason. 1974. "Animal Tissue Techniques." *Transactions of the American Microscopical Society*. https://doi.org/10.2307/3225318.

Dean, Dylan M., Anthony P. Napolitano, Jacquelyn Youssef, and Jeffrey R. Morgan. 2007. "Rods, Tori, and Honeycombs: The Directed Self-Assembly of Microtissues with Prescribed Microscale Geometries." *FASEB Journal*. https://doi.org/10.1096/fj.07-8710com.

Desroches, B R, P Zhang, B.-R. Choi, M E King, A E Maldonado, W Li, A Rago, et al. 2012. "Functional Scaffold-Free 3-D Cardiac Microtissues: A Novel Model for the Investigation of Heart Cells." *American Journal of Physiology - Heart and Circulatory Physiology* 302 (10): H2031–42. https://doi.org/10.1152/ajpheart.00743.2011.

Duckworth, A R, G A Samples, A E Wright, and S A Pomponi. 2004. "In Vitro Culture of the Ascidian Ecteinascidia Turbinata to Supply the Antitumor Compounds Ecteinascidins." *Aquaculture* 241 (1–4): 427–39. https://doi.org/10.1016/j.aquaculture.2004.08.024.

Feidantsis, Konstantinos, Basile Michaelidis, Dionysios Raitsos, and Dimitris Vafidis. 2020. "Seasonal Cellular Stress Responses of Commercially Important Invertebrates at Different Habitats of the North Aegean Sea." *Comparative Biochemistry and Physiology -Part A : Molecular and Integrative Physiology*.

https://doi.org/10.1016/j.cbpa.2020.110778.

Feng, Gen Sheng. 1999. “Shp-2 Tyrosine Phosphatase: Signaling One Cell or Many.” *Experimental Cell Research*. https://doi.org/10.1006/excr.1999.4668.

Franchi, Nicola, and Loriano Ballarin. 2017. “Immunity in Protochordates: The Tunicate Perspective.” *Frontiers in Immunology*. https://doi.org/10.3389/fimmu.2017.00674.

Fujimura, Miyuki, and Katsumi Takamura. 2000. “Characterization of an Ascidian DEAD-Box Gene, Ci-DEAD1: Specific Expression in the Germ Cells and Its MRNA Localization in the Posterior-Most Blastomeres in Early Embryos.” *Development Genes and Evolution*. https://doi.org/10.1007/s004270050012.

Hale, Alexander James, and Jeroen den Hertog. 2017. “Shp2–Mitogen-Activated Protein Kinase Signaling Drives Proliferation during Zebrafish Embryo Caudal Fin Fold Regeneration.” *Molecular and Cellular Biology*. https://doi.org/10.1128/mcb.00515-17.

Hare, Jonathan A., Wendy E. Morrison, Mark W. Nelson, Megan M. Stachura, Eric J. Teeters, Roger B. Griffis, Michael A. Alexander, et al. 2016. “A Vulnerability Assessment of Fish and Invertebrates to Climate Change on the Northeast u.s. Continental Shelf.” *PLoS ONE*. https://doi.org/10.1371/journal.pone.0146756.

Hunter, Elizabeth Sage, Christopher Paight, and Christopher E. Lane. 2020. “Metabolic Contributions of an Alphaproteobacterial Endosymbiont in the Apicomplexan Cardiosporidium Cionae.” *Frontiers in Microbiology*. https://doi.org/10.3389/fmicb.2020.580719.

Irvine, Steven Q., Katherine B. McNulty, Evelyn M. Siler, and Rose E. Jacobson. 2019. "High Temperature Limits on Developmental Canalization in the Ascidian Ciona Intestinalis." *Mechanisms of Development* 157 (June): 10–21. https://doi.org/10.1016/J.MOD.2019.04.002.

Jaenen, V., S. Fraguas, K. Bijnens, M. Heleven, T. Artois, R. Romero, K. Smeets, and F. Cebrià. 2021. "Reactive Oxygen Species Rescue Regeneration after Silencing the MAPK–ERK Signaling Pathway in Schmidtea Mediterranea." *Scientific Reports*. https://doi.org/10.1038/s41598-020-79588-1.

Jang, Ji Yong, Ji Hyun Min, Yun Hee Chae, Jin Young Baek, Su Bin Wang, Su Jin Park, Goo Taeg Oh, Sang Hak Lee, Ye Shih Ho, and Tong Shin Chang. 2014. "Reactive Oxygen Species Play a Critical Role in Collagen-Induced Platelet Activation via Shp-2 Oxidation." *Antioxidants and Redox Signaling*. https://doi.org/10.1089/ars.2013.5337.

Kawamura, K, and S Fujiwara. 1995. "ESTABLISHMENT OF CELL-LINES FROM MULTIPOTENT EPITHELIAL SHEET IN THE BUDDING TUNICATE, POLYANDROCARPA-MISAKIENSIS." *CELL STRUCTURE AND FUNCTION* 20 (1): 97–106.

Kawamura, K, S Takeoka, S Takahashi, and T Sunanaga. 2006. "In Vitro Culture of Mesenchymal Lineage Cells Established from the Colonial Tunicate Botryllus Primigenus." *ZOOLOGICAL SCIENCE* 23 (3): 245–54. https://doi.org/10.2108/zsj.23.245.

Lema, Carolina, Armando Varela-Ramirez, and Renato J Aguilera. 2011. "Differential

Nuclear Staining Assay for High-Throughput Screening to Identify Cytotoxic Compounds." *Current Cellular Biochemistry* 1 (1): 1–14. https://pubmed.ncbi.nlm.nih.gov/27042697.

Lopez, Chelsea E., Hannah C. Sheehan, David A. Vierra, Paul A. Azzinaro, Thomas H. Meedel, Niall G. Howlett, and Steven Q. Irvine. 2017. "Proteomic Responses to Elevated Ocean Temperature in Ovaries of the Ascidian Ciona Intestinalis." *Biology Open*. https://doi.org/10.1242/bio.024786.

Lorca, Rebeca, Luca Pannone, Elías Cuesta-Llavona, Gianfranco Bocchinfuso, Julian Rodríguez-Reguero, Giovanna Carpentieri, Inés Hernando, et al. 2020. "Compound Heterozygosity for PTPN11 Variants in a Subject with Noonan Syndrome Provides Insights into the Mechanism of SHP2-Related Disorders." *Clinical Genetics*. https://doi.org/10.1111/cge.13904.

Meng, Tzu Ching, Toshiyuki Fukada, and Nicholas K. Tonks. 2002. "Reversible Oxidation and Inactivation of Protein Tyrosine Phosphatases in Vivo." *Molecular Cell*. https://doi.org/10.1016/S1097-2765(02)00445-8.

Morgan, B A, J C Izpisua-Belmonte, D Duboule, and C J Tabin. 1992. "Targeted Misexpression of Hox-4.6 in the Avian Limb Bud Causes Apparent Homeotic Transformations [See Comments]." *Nature* 358 (6383): 236–39.

Napolitano, Anthony P., Dylan M. Dean, Alan J. Man, Jacquelyn Youssef, Don N. Ho, Adam P. Rago, Matthew P. Lech, and Jeffrey R. Morgan. 2007. "Scaffold-Free Three-Dimensional Cell Culture Utilizing Micromolded Nonadhesive Hydrogels." *BioTechniques*. https://doi.org/10.2144/000112591.

Neel, Benjamin G., Haihua Gu, and Lily Pao. 2003. “The ’Shp’ing News: SH2 Domain-Containing Tyrosine Phosphatases in Cell Signaling.” *Trends in Biochemical Sciences*. https://doi.org/10.1016/S0968-0004(03)00091-4.

Okada, Toshiaki, and Masamichi Yamamoto. 1993. “Identification of Early Oogenetic Cells in the Solitary Ascidians, Ciona Savignyi and Ciona Intestinalis: An Immunoelectron Microscopic Study: Oogonium/Oocyte/Germ Cell/Monoclonal Antibody/Ultrastructure.” *Development, Growth & Differentiation*. https://doi.org/10.1111/j.1440-169X.1993.00495.x.

———. 1999. “Differentiation of the Gonad Rudiment into Ovary and Testis in the Solitary Ascidian, Ciona Intestinalis.” *Development Growth and Differentiation*. https://doi.org/10.1046/j.1440-169X.1999.00471.x.

Orrego-González, Eduardo, Carlos Martin-Restrepo, and Alberto Velez-Van-Meerbeke. 2021. “Noonan Syndrome with Multiple Lentigines and PTPN11 Mutation: A Case with Intracerebral Hemorrhage.” *Molecular Syndromology*. https://doi.org/10.1159/000512374.

Parrinello, Daniela, Maria A. Sanfratello, Aiti Vizzini, and Matteo Cammarata. 2015. “The Expression of an Immune-Related Phenoloxidase Gene Is Modulated in Ciona Intestinalis Ovary, Test Cells, Embryos and Larva.” *Journal of Experimental Zoology Part B: Molecular and Developmental Evolution*. https://doi.org/10.1002/jez.b.22613.

Parrinello, Daniela, Maria Antonietta Sanfratello, Maria Giovanna Parisi, Aiti Vizzini, and Matteo Cammarata. 2018. “In the Ovary of Ciona Intestinalis (Type A),

Immune-Related Galectin and Phenoloxidase Genes Are Differentially Expressed by the Follicle Accessory Cells." *Fish and Shellfish Immunology*. https://doi.org/10.1016/j.fsi.2017.11.023.

Peddie, Clare M., Andrew C. Richest, and Valerie J. Smith. 1995. "Proliferation of Undifferentiated Blood Cells from the Solitary Ascidian, Ciona Intestinalis in Vitro." *Developmental and Comparative Immunology*. https://doi.org/10.1016/0145-305X(95)00027-Q.

Rabinowitz, C, and B Rinkevich. 2004. "Epithelial Cell Cultures from Botryllus Schlosseri Palleal Buds: Accomplishments and Challenges." *Methods in Cell Science* 25 (3–4): 137–48. https://doi.org/10.1007/s11022-004-2087-9.

Raftos, D A, D L Stillman, and E L Cooper. 1990. "In Vitro Culture of Tissue from the Tunicate Styela Clava." *In Vitro Cellular and Developmental Biology - Animal* 26 (10): 962–70. https://doi.org/10.1007/BF02624470.

Rahman, Md Sadequr, and Md Saydur Rahman. 2020. "Effects of Elevated Temperature on Prooxidant-Antioxidant Homeostasis and Redox Status in the American Oyster: Signaling Pathways of Cellular Apoptosis during Heat Stress." *Environmental Research*. https://doi.org/10.1016/j.envres.2020.110428.

Rinkevich, B. 1999. "Cell Cultures from Marine Invertebrates: Obstacles, New Approaches and Recent Improvements." *JOURNAL OF BIOTECHNOLOGY* 70 (1–3): 133–53. https://doi.org/10.1016/S0168-1656(99)00067-X.

Rinkevich, B, and C Rabinowitz. 1993. "IN-VITRO CULTURE OF BLOOD-CELLS FROM THE COLONIAL PROTOCHORDATE BOTRYLLUS-SCHLOSSERI." *In Vitro Cellular &*

Developmental Biology-Animal 29A (1): 79–85.

———. 1997. “Initiation of Epithelial Cell Cultures from Palleal Buds of Botryllus Schlosseri, a Colonial Tunicate.” *IN VITRO CELLULAR & DEVELOPMENTAL BIOLOGY-ANIMAL* 33 (6): 422–24.

Rinkevich, Baruch. 2011. “Cell Cultures from Marine Invertebrates: New Insights for Capturing Endless Stemness.” *Marine Biotechnology*. https://doi.org/10.1007/s10126-010-9354-3.

Romano, Alicia A., Judith E. Allanson, Jovanna Dahlgren, Bruce D. Gelb, Bryan Hall, Mary Ella Pierpont, Amy E. Roberts, Wanda Robinson, Clifford M. Takemoto, and Jacqueline A. Noonan. 2010. “Noonan Syndrome: Clinical Features, Diagnosis, and Management Guidelines.” *Pediatrics*. https://doi.org/10.1542/peds.2009-3207.

Rosner, Amalia, Jean Armengaud, Loriano Ballarin, Stéphanie Barnay-Verdier, Francesca Cima, Ana Varela Coelho, Isabelle Domart-Coulon, et al. 2021. “Stem Cells of Aquatic Invertebrates as an Advanced Tool for Assessing Ecotoxicological Impacts.” *Science of the Total Environment*. https://doi.org/10.1016/j.scitotenv.2020.144565.

Rowley, Andrew F. 1981. “The Blood Cells of the Sea Squirt, Ciona Intestinalis: Morphology, Differential Counts, and in Vitro Phagocytic Activity.” *Journal of Invertebrate Pathology*. https://doi.org/10.1016/0022-2011(81)90060-4.

Satoh, N, and M Levine. 2005. “Surfing with the Tunicates into the Post-Genome Era.” *Genes & Development* 19 (20): 2407–11.

https://doi.org/10.1101/gad.1365805.

Satoh, Noriyuki. 1994. *Developmental Biology of Ascidians*. Cambridge University Press.

Sawada, T, J Zhang, and E L Cooper. 1994. “SUSTAINED VIABILITY AND PROLIFERATION OF HEMOCYTES FROM THE CULTURED PHARYNX OF STYELA-CLAVA.” *MARINE BIOLOGY* 119 (4): 597–603. https://doi.org/10.1007/BF00354323.

Simmen, Martin W., Sabine Leitgeb, Victoria H. Clark, Steven J.M. Jones, and Adrian Bird. 1998. “Gene Number in an Invertebrate Chordate, Ciona Intestinalis.” *Proceedings of the National Academy of Sciences of the United States of America*. https://doi.org/10.1073/pnas.95.8.4437.

Stolfi, Alberto, and Lionel Christiaen. 2012. “Genetic and Genomic Toolbox of the Chordate Ciona Intestinalis.” *Genetics*. https://doi.org/10.1534/genetics.112.140590.

Tajan, Mylène, Audrey de Rocca Serra, Philippe Valet, Thomas Edouard, and Armelle Yart. 2015. “SHP2 Sails from Physiology to Pathology.” *European Journal of Medical Genetics*. https://doi.org/10.1016/j.ejmg.2015.08.005.

Takahashi, Hiroki, Kohji Hotta, Albert Erives, Anna Di Gregorio, Robert W. Zeller, Michael Levine, and Nori Satoh. 1999. “Brachyury Downstream Notochord Differentiation in the Ascidian Embryo.” *Genes and Development*. https://doi.org/10.1101/gad.13.12.1519.

Takamura, Katsumi, Miyuki Fujimura, and Yasunori Yamaguchi. 2002. “Primordial

Germ Cells Originate from the Endodermal Strand Cells in the Ascidian Ciona Intestinalis." *Development Genes and Evolution*. https://doi.org/10.1007/s00427-001-0204-1.

Tomanek, Lars. 2014. "Proteomics to Study Adaptations in Marine Organisms to Environmental Stress." *Journal of Proteomics*. https://doi.org/10.1016/j.jprot.2014.04.009.

Yamamoto, Masamichi, and Toshiaki Okada. 1999. "Origin of the Gonad in the Juvenile of a Solitary Ascidian, Ciona Intestinalis." *Development Growth and Differentiation*. https://doi.org/10.1046/j.1440-169x.1999.00410.x.

Zanetti, L, F Ristoratore, M Francone, S Piscopo, and E R Brown. 2007. "Primary Cultures of Nervous System Cells from the Larva of the Ascidian Ciona Intestinalis." *J. Neurosci. Methods* 165: 191–97.

Zeng, Fan, Julia Wunderer, Willi Salvenmoser, Michael W. Hess, Peter Ladurner, and Ute Rothbächer. 2019. "Papillae Revisited and the Nature of the Adhesive Secreting Collocytes." *Developmental Biology*. https://doi.org/10.1016/j.ydbio.2018.11.012.

Zheng, Hong, Shanhu Li, Peter Hsu, and Cheng Kui Qu. 2013. "Induction of a Tumor-Associated Activating Mutation in Protein Tyrosine Phosphatase Ptpn11 (Shp2) Enhances Mitochondrial Metabolism, Leading to Oxidative Stress and Senescence." *Journal of Biological Chemistry*. https://doi.org/10.1074/jbc.M113.462291.